

2021 Symposium of the Pacific Northwest Chapter of the AVS



September 8-10, 2021

**Hybrid Onsite-Virtual Meeting hosted by
Oregon State University
Corvallis OR, 97331**

Call for Student/Postdoc/Scientist Presentation/Poster Abstracts
Abstracts are due by September 3, 2021
Meeting registration opens: August 10, 2021

Contact: Zhenxing Feng, PNWAVS Chair
Email: zhenxing.feng@oregonstate.edu



The 32nd Annual Symposium of the PNWAVS Science and Technology Society (www.pnwavs.org) will be a hybrid onsite-virtual meeting hosted by Oregon State University located at Johnson Hall in Corvallis, OR. The meeting will consist of one afternoon tutorial talks and one and half days of invited talks, plenary speakers, and a student presentation competition. The onsite meeting will be hosted in Johnson 102 in Johnson Hall.

The PNWAVS symposium has a long tradition of providing a stimulating interdisciplinary program in a relaxed, informal atmosphere. The meeting attracts a broad representation of government, corporate, and university researchers from throughout the Pacific Northwest, Western Canada and Alaska. The symposium provides an excellent opportunity for students and postdocs to sharpen their presentation skills. This tradition will continue as we adopt a hybrid online-virtual format for the 2021 Symposium due to the Coronavirus pandemic. We invite oral and poster presentations from students, postdoctoral and researchers. Student presentations will be evaluated separately, and awards will be announced at the end of the symposia.

2021 PNWAVS Agenda

September 8, 2021 (Wednesday) Afternoon			
Zoom: https://oregonstate.zoom.us/j/98888234695?pwd=dGV5SblRZRmpBU1pzUFVraHZUa1B1Zz09			
Meeting ID: 988 8823 4695; Password: 046578			
13:15-13:20	Zhenxing Feng	Greetings	Oregon State University
13:20-13:30	Gregory Herman	Opening Remarks	Oregon State University
Session 1: NNCI/Characterization Tutorial. Chair: Zhenxing Feng			
13:30-14:10	Heath Kersell	(Invited) Chemical and Nanoscale Structural Probes in Ambient Pressures: A Practical Tutorial in AP-XPS and AP-STM	Oregon State University
14:10-14:50	Dan Graham	(Invited) ToF-SIMS: Solving problems and answering questions by blowing things up	University of Washington
14:50-15:20	Break		
15:20-16:00	John Conley	(Invited) Atomic Layer Deposition and the OSU Materials Synthesis and Characterization (MaSC) Center	Oregon State University
Session 2: Students Presentations. Chair: Thevuthasan Suntharampillai			
16:00-16:15	Joel Price**	An optical study of LaNiFeO ₃	Eastern Washington University
16:15-16:30	William Guo***	Techno-economic Comparison of Catalysts for Proton-Exchange Membrane Electrolysis	Lincoln High School
16:30-16:45	Marcus A. Sharp*	Study of Rh Adatoms, Nanoparticles, and Mixed Oxide Systems on the Single Crystal Fe ₃ O ₄ (001) Surface in UHV	Pacific Northwest National Laboratory
16:45-17:00	Ariel Whitten*	Deconvoluting XPS Spectra in Lanthanum-Based Perovskites: An Analysis from First Principles	Washington State University
17:00-17:15	Hoan Nguyen*	Synergistic Study of Thermal Decomposition of Acetic Acid on Pd(111) using Ambient Pressure X-Ray Photoelectron Spectroscopy (AP-XPS) and Density Functional Theory (DFT)	Oregon State University
17:15-17:30	Yadong Zhou*	Revealing of mixing states of aerosol particles using 3-dimensional mass spectrometric imaging analysis	Pacific Northwest National Laboratory
17:30-17:45	Youngjoon Hong*	Design and Fabrication of Cost-Effective Systems for Atomic Layer Deposition	Oregon State University
17:45-18:00	Break		
Plenary Session (I). Chair: Elton Graugnard			
18:00	Reception/Dinner		
18:30-19:20	Andrei Kolmakov	(Plenary) Interfacial Spectroscopy, Imaging, and Fabrication in Liquids with Electron and X-ray beams	National Institute of Standards and Technology

September 9, 2021 (Thursday) Morning

Zoom: <https://oregonstate.zoom.us/j/92291154798?pwd=Tjl4dTZ2UWxING1xZUY1T2hVV2V2Zz09>

Meeting ID: 922 9115 4798; Password: 138060

Session 3: Growth and Characterizations I. Chair: Zhenxing Feng

8:00-8:40	Tristan Petit	(Invited) Soft X-ray spectroscopy at the solid-water interface of nanomaterials	Helmholtz-Zentrum Berlin, Germany
8:40-8:55	Marcos Lucero*	High performance iron-based phosphate anode for aqueous sodium-ion batteries	Oregon State University
8:55-9:10	Mayur Pole*	Characterization and Surface Deformation Behavior of Cu/Nb Nano Layered Composites	Pacific Northwest National Laboratory
9:10-9:25	Alvin Chang*	Quantitative Measure of 3D Nanostructure and Size Dispersity of Ultrasmall Fluorescent Silica Nanorings via Small-Angle X-ray Scattering	Cornell University
9:25-9:40	Cheng-Han Li*	In situ AFM Study of Electrochemical Corrosion in FeCrNi Alloy in Deuterium Chloride Solution	Pacific Northwest National Laboratory
9:40-9:55	V. Vinay K. Doddapaneni*	Additive Manufacturing of Nanostructured Tungsten Coatings for Solar-Thermal Applications	Oregon State University
9:55-10:30	Break		

Session 4: Growth and Characterizations II. Chair: Tiffany Kaspar

10:30-11:10	Matthew Yankowitz	(Invited) Strong correlations and topology in graphene-based moiré quantum materials	University of Washington
11:10-11:25	Pritha Biswas*	Oxygen Vacancy Induced Polymorphs Formation in RF Sputtered TiO ₂ and Widening of Stability Window of Low Temperature Polymorph	Oregon State University
11:25-11:40	Kevin D. Vallejo*	Tensile-strained InGaAs quantum dots on GaSb(111)A via molecular beam epitaxy	Boise State University
11:40-11:55	Anqi Yu*	Decoupling of Strain and Temperature Effects on Microstructural Evolution during High Shear Strain Deformation	Pacific Northwest National Laboratory
11:55-12:10	Jake Soares*	Nucleation and growth of molybdenum disulfide grown by thermal atomic layer deposition on metal oxides	Boise State University
12:10-12:25	Carrington Moore*	Determining the Adsorption Mechanism of 2,3-butanediol on	Washington State University

		RuO ₂ using First Principles Calculations Coupled with Global Optimizers	
12:25-13:30	Boxed Lunch		

September 9, 2021 (Thursday) Afternoon			
Zoom: https://oregonstate.zoom.us/j/92291154798?pwd=Tjl4dTZ2UWxING1xZUY1T2hVV2V2Zz09			
Meeting ID: 922 9115 4798; Password: 138060			
Plenary Session (II). Chair: Xiao-Ying Yu			
12:40-13:30	Jinghua Guo	(Plenary) In-situ/operando soft x-ray spectroscopy of chemical and catalytic interfaces	Lawrence Berkeley National Laboratory
Session 5: Biology and Environmental Study I. Chair: Xiao-Ying Yu			
13:30-14:10	Luke Hanley	(Invited) Microbial Phenotype Probed by Mass Spectrometry: From Bottom Up Proteomics to Metabolite Imaging	University of Illinois at Chicago
Poster Session			
14:10-15:30	Gather.Town	https://gather.town/app/wuuiYqMLZqDGBcph/PNWAVS2021	
15:30-16:00	Break		
Session 6: Energy Applications I. Chair: Mark Engelhard			
16:00-16:40	Liane Moreau	(Invited) Mapping the effects of physical and chemical reduction parameters on local atomic distributions within bimetallic nanocrystals	Washington State University
16:40-16:55	Widitha Samarakoon*	Structure and Properties of Epitaxial LiCoO ₂ thin films	Oregon State University/PNNL
16:55-17:10	Si-Hao Chen*	Cu-Ga-S/ZnS Quantum Dots with Silica Melting Gel as a Luminescent Downshifting Coating for Enhancing Solar Photovoltaic Power Generation	Oregon State University
17:10-17:25	Nasseha Cardwell*	Capturing the Coverage Dependence of Aromatics via Mean-Field Models	Washington State University
17:25-17:40	Jack Grimm*	Characterization of the composition and mechanical properties of aprismatic crocodilian tooth enamel	University of Washington
17:40-17:55	Susan Mathai*	Aerosol properties and processing during wintertime under hazy condition	Pacific Northwest National Laboratory
18:00	Dinner		

Poster Session, September 9, 2021 (Thursday) 14:10-15:30

<https://gather.town/app/wuuiYqMLZqDGBcph/PNWAVS2021>

Poster 1	Luke Soule	Understanding the Role of Aliovalent Al Doping at the Mg Metal Battery Interface using Operando and In-situ Spectroscopy	Pacific Northwest National Laboratory
Poster 2	Cole DeCesare**	Characterization and Confirmation of Products of Zeolitic Imidazolate Framework 8 (ZIF-8) Thin-Film, Room-Temperature, Microfluidic Pen Synthesis	Oregon State University
Poster 3	Beckett Lewis**	Controlling the Morphology of Vapor Phase Deposition of Tungsten by Different Heating Techniques	Oregon State University
Poster 4	Jeffrey Dhas*	Inkjet Printed Europium-doped Yttria for Anti-Counterfeiting on Stainless Steel and Glass	Oregon State University
Poster 5	Jessica Jenkins*	Reaction of 2-Propanol on SnO ₂ (101) Studied using Ambient-Pressure X-ray Photoelectron Spectroscopy	Oregon State University
Poster 6	Zachary Evans*	Effects of Lattice Hydrogen Concentration on Ammonia Synthesis	Oregon State University
Poster 7	Han Mei*	Continuous flow synthesized nanoparticles	Oregon State University
Poster 8	Abu Sayeed Md Shawon*	Understanding Cloud Condensation Activity of Aerosol with Higher Temporal Resolution	Michigan Technological University/PNNL

September 10, 2021 (Friday) Morning			
Zoom: https://oregonstate.zoom.us/j/98450197786?pwd=NVDlQ255d1p4S0plK1U2OHJuTnpHZz09			
Meeting ID: 984 5019 7786; Password: 315061			
Session 7: Energy Applications II. Chair: Chih-hung Chang			
8:30-9:10	Konstantinos Goulas	(Invited) Deciphering electronic and geometric effects in bimetallic catalysis for biomass upgrading	Oregon State University
9:10-9:25	Kingsley Chukwu	Effects of aprotic and polar co-adsorbates on C-OH and O-H bond cleavages on Pd (111)	Oregon State University
9:25-9:40	Le Wang	Understanding the Electronic Structure Evolution of Epitaxial $\text{LaNi}_{1-x}\text{Fe}_x\text{O}_3$ Thin Films for Water Oxidation	Pacific Northwest National Laboratory
9:40-9:55	Shujie Li	Inkjet-Printed p-type $\text{CuBr}_x\text{I}_{1-x}$: A Wide-Range-Tunable Resistivity of wearable thin-film transistors	Oregon State University
9:55-10:10	Jiyoung Song	Making electrodes by particle stamping for microscopic and electrochemical analysis	Pacific Northwest National Laboratory
10:10-10:30	Break		
Session 8: Biology and Environmental Study II. Chair: Vaithiyalingam Shutthanandan			
10:30-11:10	Swarup China	(Invited) Chemical imaging of atmospheric particles from wildfire smoke	Pacific Northwest National Laboratory
11:10-11:25	Peter Moeck	Objective crystallographic symmetry classifications of atomic and molecular resolution images from crystals in direct and Fourier space	Portland State University
11:25-11:40	Jun Gao	Revealing the material interface compatibility between CO_2 separation membrane and water-lean solvents using ToF-SIMS	Pacific Northwest National Laboratory
11:40-11:55	Lyndi E. Strange	Understanding the Effects of Surface treatment on the Boehmite Layer of Al-6061	Pacific Northwest National Laboratory
11:55-12:40	Award Ceremony and closing remarks		
12:40-14:00	Boxed lunch and PNWAVS Chapter Board Meeting (Different Zoom Links)		
13:30 Tour to ATAMI and APSLC labs, part of NNCI facilities (onsite only)			
* = Graduate student; ** = Undergraduate student *** = High School Student			

September 8, 2021 (Wednesday) 13:15-13:20
Zhenxing Feng: Chairman Greetings

September 8, 2021 (Wednesday) 13:20-13:30
Gregory Herman, School Head of Chemical, Biological, and Environmental Engineering: Opening Remarks

Session 1: NNCI/Characterization Tutorial. Chair: Zhenxing Feng
September 8, 2021 (Wednesday) 13:30-14:10
Chemical and Nanoscale Structural Probes in Ambient Pressures: A Practical Tutorial in AP-XPS and AP-STM (Invited)

Heath Kersell¹

heath.kersell@oregonstate.edu

¹. School of Chemical, Biological and Environmental Engineering, Oregon State University, Corvallis, OR, USA

As dimensions reach the nanoscale, a rich interplay between chemistry and structure often profoundly influences material function. For example, adsorbate-surface interactions at solid-gas interfaces can yield nanocluster formation, subsurface species segregation, oxidations or reductions, surface constituent diffusion, and other processes resulting from or even driving chemical activity. While a number of surface science techniques have been modified for ambient pressure investigations, understanding the relationship between structure, chemistry, and function in ambient gas environments remains a challenge.

A successful approach to understanding the correlation between chemical transitions and structural transformations in ambient conditions has been to combine ambient pressure X-ray photoelectron spectroscopy (APXPS) with ambient pressure scanning tunneling microscopy (APSTM). This tutorial will introduce these two techniques in the context of ambient pressure studies which they are uniquely suited to. Different types of APXPS and APSTM systems, their capabilities, and considerations/limits for their use will be discussed. Additionally, a brief overview of data analysis and gas phase processes observed in APXPS and APSTM will be provided. All topics discussed will be motivated by examples of research enabled by these techniques. For example, a discussion of peak fitting in APXPS will be accompanied by an example of its use identifying surface species and the evolution of surface compositions. APSTM analysis will be discussed in the context of understanding structural transformations in ambient gas environments.

It is hoped that newcomers to the field can benefit from the broad overview of these topics, while experienced practitioners will find examples of application informative. Finally, I will briefly survey several user facilities where these techniques can be accessed through various proposal processes by interested groups.

September 8, 2021 (Wednesday) 14:10-14:50

ToF-SIMS: Solving problems and answering questions by blowing things up (Invited)

Daniel J. Graham^{1,2}

Corresponding Author: djgraham@uw.edu

¹. NESAC/BIO, University of Washington, Department of Bioengineering, Seattle, WA, USA.

². Molecular Analysis Facility, University of Washington, Seattle, WA, USA.

<https://www.moles.washington.edu/maf/>

Surfaces play a critical role in almost all aspects of our lives. They are involved in the interactions that control processes ranging from the biological functions of cells and tissues to chemical reactions that enable solar cells and non-fouling coatings. This means that it is critical to know as much as possible about a surface in order to both understand the interactions that occur and to be able to design surfaces that promote successful interactions. Time-of-flight secondary ion mass spectrometry (ToF-SIMS) is a powerful surface analytical method that has been proven to provide valuable, molecular specific information about a wide range of surfaces. ToF-SIMS generates detailed spectra that contain signals from both intact molecules and molecular fragments that can encode information about the identity and arrangement of surface molecules. ToF-SIMS has very high sensitivity and can often detect species in the ppm or ppb range. In addition, modern ToF-SIMS instruments can generate 2D images with lateral resolutions below 1 micron and 3D images with depth resolutions below 10 nm. In order to maximize the information gained from ToF-SIMS, it is important to understand how to properly handle and prepare samples and how to optimize an experimental plan. In this tutorial I will present background information and suggested guidelines for the application of ToF-SIMS to wide range of materials. This is aimed at being a practical guide to help you understand the basics of ToF-SIMS and provide an introduction on collecting and analyzing data when working with ToF-SIMS. Examples will be provided to demonstrate the detailed chemical information that ToF-SIMS can provide to help solve problems and answer research questions.

September 8, 2021 (Wednesday) 14:20-16:00

Break

September 8, 2021 (Wednesday) 15:20-16:00

Atomic Layer Deposition and the OSU Materials Synthesis and Characterization (MaSC) Center (Invited)

John F. Conley, Jr.

jconley@eecs.oregonstate.edu

School of EECS, Oregon State University, Corvallis, OR, 97331

Atomic layer deposition (ALD) is a special type of chemical vapor deposition based on sequential, self-saturating surface reactions, separated by inert gas purges. This full reaction cycle sequence is repeated until the desired thickness is reached. Deposition thus proceeds in a layer by layer manner, with less than a monolayer of material per cycle. Thickness is controlled by the number of reaction cycles, rather than the reaction time. The benefits of ALD include atomic scale thickness and composition control, excellent uniformity and conformality, even over complex substrates, and high film quality at relatively low deposition temperatures. Originally developed in the mid-1970's in Finland for application to flat panel electroluminescent displays, atomic layer deposition (ALD) is now critical in the semiconductor industry and is finding application in batteries, solar cells, biomedical devices, conformal barrier coatings, etc. The first part of this invited talk will cover the fundamentals atomic layer deposition (ALD), highlight some of the recent applications of ALD at OSU, describe current areas of research, and point towards future directions in the field. In the second part, the capabilities of the Materials Synthesis and Characterization (MaSC) Center at OSU will be overviewed.

Session 2: Students Presentations. Chair: Thevuthasan Suntharampillai
September 8, 2021 (Wednesday) 16:00-16:15
An optical study of LaNiFeO_3

Joel Price¹

Corresponding Author: pricejb94@gmail.com

¹. Eastern Washington University, Cheney, WA United States

A spectroscopic ellipsometry analysis of samples of $\text{LaNi}_{1-x}\text{Fe}_x\text{O}_3$ showed that, when iron concentration was adjusted, the electronic properties shifted. With the use of a J. A. Woollam spectroscopic ellipsometer, the optical characteristics were mapped out for several nickel-iron combinations in the perovskite matrix. This lends insight into the uses of these materials in semiconductor applications. The base material, LaNiO_3 is a perovskite that is useful in a wide variety of applications, because it remains metallic over a wide range of temperatures without transitioning to an insulator. LaFeO_3 has implementation as a semiconductor in many areas. The perovskite material, $\text{LaNi}_{1-x}\text{Fe}_x\text{O}_3$, is of particular interest, due to its ability to have its electronic properties altered by adjusting the concentration of iron atoms. A spectrometric analysis of several samples of $\text{LaNi}_{1-x}\text{Fe}_x\text{O}_3$, varying from x values of zero to one, shows that the electronic properties, including the absorption coefficient, refractive index, and band gap, can be controlled via this method. It was found to be metallic up to an iron concentration of 0.5, at which point it changed to a semiconductor.

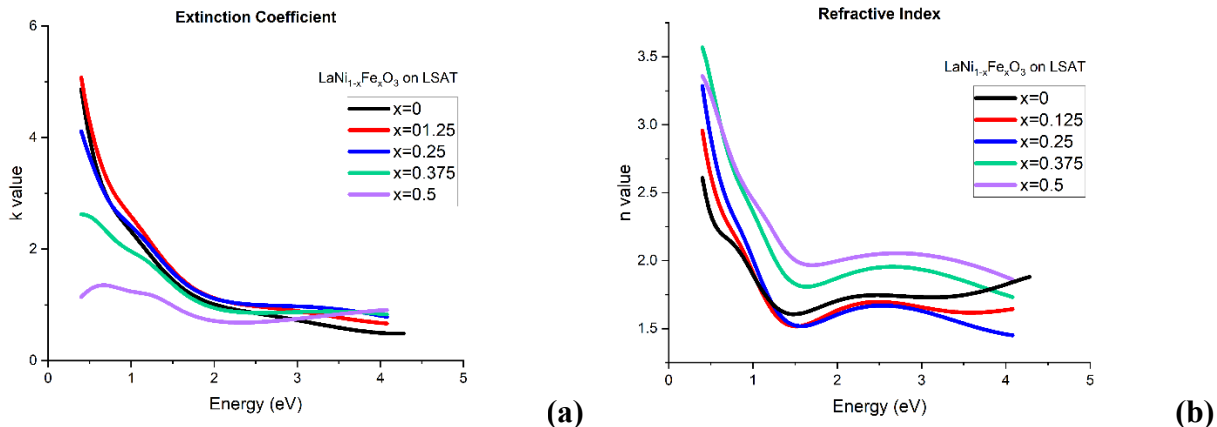


Figure 1 (a) Extinction coefficient **(b)** Index of refraction

References:

- [1] H. Tompkins, and J. Hilfiker. Ellipsometry: Practical Application to Thin Film Characterization, Momentum Press, LLC, 2016, Chap. 2, pp. 11-28.
- [2] M. D. Scafetta, *et al.*, J. Phys. Condensed Matter, 26 505502 (2014)
- [3] I wish to acknowledge the sponsor for this research: the United States Department of Energy through the WDTS visiting faculty program. I also wish to acknowledge the Pacific Northwest National Laboratory for facilitating this research.

September 8, 2021 (Wednesday) 16:15-16:30

Techno-economic Comparison of Catalysts for Proton-Exchange Membrane Electrolysis

William Guo¹, Zhenxing Feng²

Corresponding Author: zhenxing.feng@oregonstate.edu

¹ Lincoln High School, Portland, OR, USA

² School of Chemical Biological, and Environmental Engineering, Oregon State University, Corvallis, OR, USA

Water electrolysis as a method for energy production has received significant attention in recent years due to its sustainable hydrogen production capabilities and potential competitiveness with fossil fuels if coupled with renewable energy sources. In particular, proton exchange membrane (PEM) electrolysis has emerged as an efficient and versatile technology that can operate at high current densities. The primary focus of research has been on finding effective, low-cost catalysts for the oxygen evolution reaction (OER), since the high overpotential of this reaction has been the limiting factor in the widespread commercialization of PEM electrolyzers. I conducted a literature review and developed a techno-economic model for state-of-the-art PEM electrolysis across different catalysts, and compared the findings with other hydrogen production methods, such as anion exchange membrane (AEM) electrolysis and steam methane reforming using fossil fuels. Current hydrogen produced from PEM electrolysis costs \$5-\$6/kg-H₂, substantially higher than steam methane reforming (SMR) H₂ costs of \$1.34-\$2.20/kg. Commercial electrolyzers use

platinum-group catalysts that operate at current densities around 2 A/cm² and overpotentials ranging from 470mV to 770mV and can be used for 60000 hrs. Catalyst research has found that iridium-based catalysts such as IrO₂, Ru_{x-1}Ir_xO₂, and SrIrO₃ have higher performance and similar lifetimes, with 340mV-440mV of overpotential at 1A/cm², at the expense of the higher cost of catalyst loading. Herein, I provide potential methods to reduce hydrogen costs and establish targets for electrocatalysts to be competitive with alternative hydrogen fuel sources.

September 8, 2021 (Wednesday) 16:30-16:45

Study of Rh Adatoms, Nanoparticles, and Mixed Oxide Systems on the Single Crystal Fe₃O₄(001) Surface in UHV.

Marcus A. Sharp^{1,2}, Chris J. Lee², Mausumi Mahapatra², R. Scott Smith², Bruce D. Kay², Zdenek Dohnálek^{1,2}

Corresponding Author: Zdenek.Dohnalek@pnnl.gov

1. Voiland School of Chemical Engineering and Bioengineering, Washington State University, Pullman, Washington 99163, USA,
2. Physical and Computational Sciences Directorate and Institute for Integrated Catalysis, Pacific Northwest National Laboratory, Richland, Washington 99354, USA

Single atom catalysts have emerged as a new frontier in catalysts due to the need for improved catalyst activity and selectivity. Unfortunately, challenges exist due to their limited stability, and understanding of their coordination environment. Surface science studies have the tools necessary to investigate such single atoms and their chemistry under well-controlled conditions, thus providing clear correlations between the active site environment and observed chemical processes. Here, we have studied the behavior of Rh on the Fe₃O₄(001) single crystal surface using X-ray photoelectron spectroscopy, temperature programmed desorption, and scanning tunneling microscopy. We employ the Fe₃O₄(001) reconstructed surface that has been shown to stabilize single 2-fold coordinated metal adatoms to elevated temperatures.¹ By varying the Rh loading and annealing temperature, we have identified a series of model catalysts possessing unique Rh sites (Figure 1). These catalysts include Rh adatoms, mixed surface layers with octahedrally-coordinated Rh, and pure metallic clusters. CO and CO₂ TPD's and STM are further used to characterize the Rh coverage, binding, and average particle size distribution. These model systems allow us to directly investigate reaction processes on different types of catalytic sites. Future studies will be directed toward studying the energetics and reaction pathways of the hydrogenation of unsaturated hydrocarbons and carbonyl functional groups.

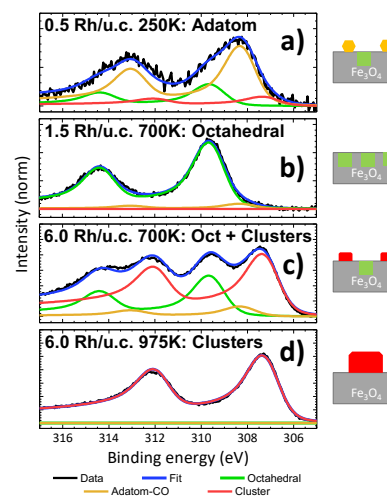


Figure 1: XPS characterization allows the identification of Rh species as a function of metal loading and annealing temperature.

References:

- [1] Jakub, Z.; Hulva, J.; Ryan, P. T. P., Adsorbate-induced structural evolution changes the mechanism of CO oxidation on a Rh/Fe₃O₄(001) model catalyst. *Nanoscale* **2020**, *12*, 5866-5875.

September 8, 2021 (Wednesday) 16:45-17:00

Deconvoluting XPS Spectra in Lanthanum-Based Perovskites: An Analysis From First Principles

Ariel Whitten¹, Elif Tezel², Dezhou Guo¹, Mahdokht Soltani¹, Reinhard Denecke³, Eranda Nikolla², Jean-Sabin McEwen¹

Corresponding Author: js.mcewen@wsu.edu

¹. Gene and Linda Voiland School of Chemical Engineering and Bioengineering, Washington State University Pullman, WA, United States of America

². College of Engineering, Wayne State University, Detroit, Michigan, 48202, United States

³. Wilhelm-Ostwald-Institute for Physical and Theoretical Chemistry, Leipzig University, Leipzig D-04103, Germany

CO₂ and H₂O co-electrolysis has the potential to create a new source of syngas using solid oxide electrolysis cells (SOECs). Perovskites are promising SOEC cathode materials due to their ability to reduce stable molecules, such as CO₂. The application of these materials in reduction reactions is limited by the lack of understanding of the underlying mechanisms. In this study, we aim to deepen the understanding of the perovskite surface structures and how they impact reactivity by deconvoluting experimental X-ray photoelectron spectroscopy. Specifically, we deconvolute the experimental XPS spectra of three La-based perovskite surfaces with different B-site cations (Ni, Fe and Co).

Our preliminary results on a LaNiO₃ (001) NiO₂-terminated surface demonstrate that a generalized gradient functional is sufficiently accurate to capture the CLBES as shown for O 1s in Figure 1. The calculations were performed in a p(2×2) unit cell to model the antiferromagnetic ground state of our systems. We find that the adsorbed oxygen species have higher core level binding energy values as compared to the surface lattice oxygen. We further find that the lattice oxygen in the subsurface layers also have higher CLBES as compared to those at the surface. These results are consistent with our corresponding experimental temperature dependent XPS results. Similar comparisons will be conducted for the LaBO₃ (B=Co, Fe) (001) BO₂-terminated surfaces with the presence of surface impurities, but excluding antiferromagnetic ordering as the RBPE function predicts the unmagnetized surface to be the ground state for these systems. Once we define our systems at ground state, we will begin

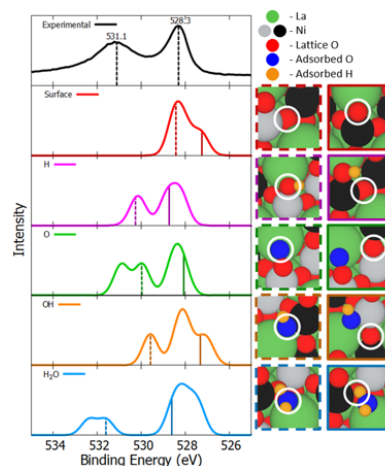


Figure 1. On the left: Top: Experimental XPS O 1s data for LaNiO₃. The graphs below depict the theoretical XPS data. The red curve depicts the spectrum of the surface without adsorbed species. The purple, green, orange, and blue curves show the spectrum of the surface with adsorbed species. On the right: Images of species contributing to each of the peaks in the presence of adsorbed atoms/molecules. The border color signifies to the energies marked on the theoretical XPS graph. The corresponding atoms are circled in white.

investigating the effects of electric fields on the CLBES to better model the electrocatalyst under operating conditions.

September 8, 2021 (Wednesday) 17:00-17:15

Synergistic Study of Thermal Decomposition of Acetic Acid on Pd(111) using Ambient Pressure X-Ray Photoelectron Spectroscopy (AP-XPS) and Density Functional Theory (DFT)

Hoan Nguyen¹, Rafik Addou¹, Kingsley Chukwu¹ and Líney Árnadóttir¹

Corresponding Author: Liney.Arnadottir@oregonstate.edu

¹. School of Chemical, Biological and Environmental Engineering, Oregon State University, Corvallis, United States of America.

Acetic acid's thermal decomposition over Pd (111) is a good model to study the decomposition of fatty acids and other oxygenates involved in biofuel production. The molecular understanding of this surface reaction could give important insights into how to tune the selectivity of the reactions. Previous density functional theory (DFT) studies on the thermal decomposition of acetic acid on Pd (111) suggest that carbon monoxide (CO) and carbon dioxide (CO₂), are produced by two different reaction pathways: decarbonylation (DCN), and decarboxylation (DCX), respectively. To further understand these reaction mechanisms, we have studied this model system using ambient pressure X-ray photoelectron spectroscopy (AP-XPS) and mass spectrometry (MS). The experimental data analysis is supported by DFT calculations of core-level binding energies (CLBEs) to deconvolute the XPS spectra. XPS analysis of Pd (111) exposed to acetic acid (at 1 mbar and room temperature) shows the presence of adventitious carbon, chemisorbed acetic acid, acetate, and CO, as well as gaseous acetic acid. We also explored the effect of co-adsorbed water on the selectivity of the decomposition by dosing acetic acid in the presence of water. The addition of waters shows an increase in the coverage of acetic acid and a decrease in CO coverage. Moreover, gaseous components from the reaction show an increase in CO₂/CO ratio from 45% to 80%, suggesting an enhancement of DCX over DCN when co-adsorbed water is present. Experimental observations are supported by calculations of the reaction's mechanism and microkinetic modeling, show that the presence of co-adsorbed water favors the DCX pathway over DCN pathway by lowering barriers for O-H bond breakings but increasing barriers for C-O bond breakage.

September 8, 2021 (Wednesday) 17:15-17:30

Revealing of mixing states of aerosol particles using 3-dimensional mass spectrometric imaging analysis

Yadong Zhou¹, Fan Mei², Zihua Zhu^{1,*}

¹ Environmental Molecular Science Laboratory, Pacific Northwest National Laboratory, Richland, WA 99354, USA

² Atmospheric Sciences and Global Change Division, Pacific Northwest National Laboratory, Richland, WA 99352, USA.

Presenter: Mr. Yadong Zhou, visiting PhD student

* Corresponding author: Zihua Zhu, zihua.zhu@pnnl.gov

Mixing states of aerosol particles are very important for understanding the role of aerosols in air quality and climate. However, determination of mixing states of the aerosol particles has been challenging, because most traditional chemical analysis tools used in this field are bulk analysis tools, which can't provide enough 3-dimensional information for the fine structure. Sophisticated imaging tools, including Scanning Electron Microscope (SEM) and Transmission Electron Microscope (TEM) can provide high spatial resolution (a few nm to sub-nm level) topographic images. However, only limited chemical information, such as bulk elemental information, is available. Time-of-flight secondary ion mass spectrometry (ToF-SIMS) is a powerful surface analysis tool. It can simultaneously provide elemental, isotopic and molecular information with part per million (ppm) sensitivity. More importantly, it is very surface sensitive, and its information depth is less than a few nanometers. Also, ToF-SIMS can perform 3-dimensional molecular imaging with decent spatial resolution (sub-micron in xy directions, and 1-5 nm in z direction). Such capabilities are unique in aerosol research. In this work, 3-dimensional ToF-SIMS imaging analysis provided critical information to elucidate the mixing states of aerosol particles. PM_{2.5} aerosol samples in a typical Beijing winter pollution case were used as a model system. Our data show that mixing states of the PM_{2.5} hardly change from low to medium pollution situations, and only single-component particles form (external mixing). Under severe pollution situation, a large amount of KNH₄SO₄ and NH₄Cl were observed. Such an observation is surprising, because in traditional theories, (NH₄)₂SO₄ and KCl should be more plausible. This finding strongly indicates that relying on the bulk properties may lead to misidentification of the effective chemical composition of aerosol particles, which may cause larger uncertainties in the estimate of Cloud condensation nuclei properties.

September 8, 2021 (Wednesday) 17:30-17:45

Design and Fabrication of Cost-Effective Systems for Atomic Layer Deposition

Youngjoon Hong¹

Corresponding Author: hongyo@oregonstate.edu

¹. School of Chemical, Biological and Environmental Engineering, Oregon State University, Corvallis, US.

Atomic Layer Deposition (ALD) is a film deposition technique, based on cyclic sequence of alternating pulses of gas phase chemical reactants, separated by purging step. ALD process offers precise control of thickness and conformal uniformity due to the self-saturating chemisorption of reactants on the substrate surface. Our ALD systems are composed of vacuum chamber, vacuum pump, heater, Quartz Crystal Microbalance (QCM), Temperature controller, Mass Flow Controller, pressure sensor, and ALD valves. Although the temperature stabilization time takes around 4 hours, our system could deposit aluminum oxide film on the Si-wafer successfully. However, the main problem of our current ALD systems is the uniformity of the deposited film

thickness (**Figure 1**). The film is deposited much thicker on the reactant inlet side than outlet side of the Si-wafer. Moreover, there was significant heat sink from heating elements to the surrounding in the vacuum chamber, and it caused unwanted chemical vapor deposition. A stepper motor is in the process of installation to improve the uniformity of the deposited film thickness by rotating the Si-wafer, and Calcium Silicate insulating board will be placed on the heating elements to minimize unwanted chemical vapor deposition by reducing the heat sink to the environments in the chamber.

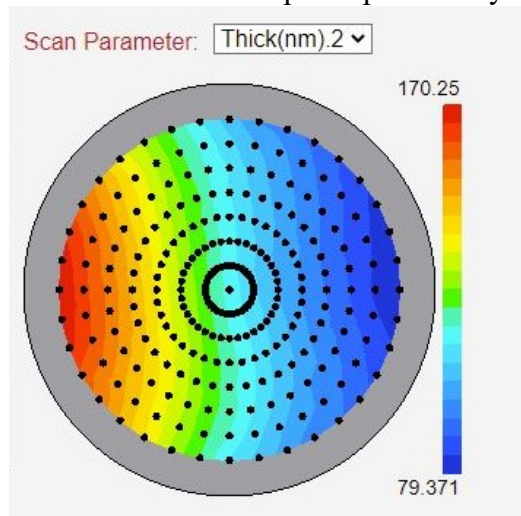


Figure 1 Contour plot of deposited Al₂O₃ thickness measure by ellipsometer

September 8, 2021 (Wednesday) 17:45-18:00

Break

Plenary Session (I): Chair: Elton Graugnard

September 8, 2021 (Wednesday) 18:30-19:20

Interfacial Spectroscopy, Imaging, and Fabrication in Liquids with Electron and X-ray beams (Plenary)

Andrei Kolmakov¹

Corresponding Author: andrei.kolmakov@nist.gov

¹ Nanoscale Device Characterization Division, NIST, Gaithersburg, MD 20899, USA

Bridging the “pressure gap” between traditional high- (and UHV)- vacuum analytical tools such as SEM, XPS, AES, PEEM and realistic sample environments is the major experimental challenge to study interfacial processes relevant to electrochemical, environmental research, catalysis and biomedical applications. The recent implementation of the nanometer-thin *electron transparent membranes* that separate the liquids or dense gases from UHV environments [1, 2] enabled the use of the standard HV (UHV) analytical instrumentation in conjunction with already existing lab-on-a-chip MEMS technologies. We first discuss multi-windows graphene liquid cells designs such as microchannel arrays (MCA)[3] and their applications for electrochemical studies[4]. Such designs allow for high throughput combinatorial spectromicroscopy data mining algorithms such as principal component analysis, clustering, Bayesian inference methods etc. We highlight the

capabilities of this membrane-based approach to perform electron spectroscopy, high resolution imaging and future trends [5]. Moreover, the solution of this “pressure and material gap” impediments enables *in-liquid* direct write technique for 3D-sculpturing of biocompatible polymer materials such as hydrogels [6]. We defined the characteristic parametric space for fine features writing energy, dwell time, which determine the ultimate feature size (resolution) and demonstrated the potential of this technique on a few selected examples such as live-cell encapsulation, and plasmonic sensing.

References:

- [1] A. Kolmakov *et al.*, "Graphene oxide windows for in situ environmental cell photoelectron spectroscopy," (in English), *Nature Nanotechnology*, vol. 6, no. 10, pp. 651-657, Oct 2011.
- [2] H. Guo *et al.*, "Enabling photoemission electron microscopy in liquids via graphene-capped microchannel arrays," *Nano letters*, vol. 17, no. 2, pp. 1034-1041, 2017.
- [3] A. Yulaev, H. Guo, E. Strelcov, L. Chen, I. Vlasiouk, and A. Kolmakov, "Graphene-capped multichannel arrays for combinatorial electron microscopy and spectroscopy in liquids," *ACS Applied Materials and Interfaces* vol. 9, no. 31, pp. 26492-26502, 2017.
- [4] S. r. Nemšák *et al.*, "Interfacial Electrochemistry in Liquids Probed with Photoemission Electron Microscopy," *Journal of the American Chemical Society*, vol. 139, no. 50, pp. 18138-18141, 2017.
- [5] S. Nemšák *et al.*, "In aqua electrochemistry probed by XPEEM: experimental setup, examples, and challenges," *arXiv preprint arXiv:1802.02545*, 2018.
- [6] T. Gupta *et al.*, "Electron and X-ray Focused Beam-Induced Cross-Linking in Liquids: Toward Rapid Continuous 3D Nanoprinting and Interfacing using Soft Materials," *ACS Nano*, vol. 14, no. 10, pp. 12982-12992, 2020.

September 9, 2021 (Thursday) Morning

Session 3: Growth and Characterizations I. Chair: Zhenxing Feng

September 9, 2021 (Thursday) 8:00-8:40

Soft X-ray spectroscopy at the solid-water interface of nanomaterials (Invited)

Tristan Petit¹

Corresponding Author: tristan.petit@helmholtz-berlin.de

¹ Helmholtz-Zentrum Berlin, Germany

The characterization of the solid-water interface in nanomaterials is essential for applications involving chemical and electronic processes in aqueous medium such as in medicine, biosensing or energy storage and conversion. In this seminar, I will introduce synchrotron-based X-ray spectroscopy techniques and explain how they can be applied to investigated solid-liquid interfaces. Example of our work on the characterization of the interface between nanodiamonds and 2D titanium carbides, so-called MXene, and water will be shown. Perspectives towards X-ray spectroscopy with nanoscale spatial resolution in liquid will then be briefly presented.

September 9, 2021 (Thursday) 8:40-8:55

High performance iron-based phosphate anode for aqueous sodium-ion batteries

Marcos Lucero¹, Shen Qiu¹, Xianyong Wu¹ and Zhenxing Feng*,

*Corresponding Author: zhenxing.feng@oregonstate.edu

1. School of Chemical, Biological, and Environmental Engineering, Oregon State University, Corvallis, OR 97331, USA

Aqueous sodium-ion batteries are a top candidate for applications such as large scale stationary energy storage where low-cost and long cycle life are the priority.¹ Lack of suitable anode materials has halted the development of this technology. We demonstrate the superior electrochemical performance of the anode $\text{Na}_3\text{Fe}_3(\text{PO}_4)_4$.² This electrode exhibits a reversible capacity of $\sim 83 \text{ mAh g}^{-1}$, excellent rate capability from 0.1 C up to 200 C ($1\text{C} = 83 \text{ mAh/g}$), and outstanding cycle life of 6000 cycles. *In-situ* synchrotron X-ray diffraction and X-ray absorption spectroscopy were utilized to understand the structural (e.g. crystal and electronic) evolution of the anode during charging-discharging processes. We find that the material undergoes small volume expansions upon sodium insertion ($\sim 3\%$) which enables fast charging and long-cycling capability.

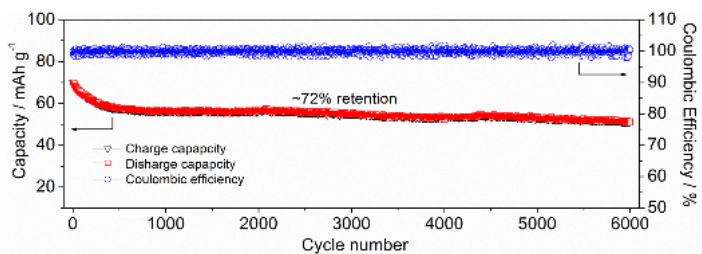


Fig. 1 | Long term electrochemical performance of $\text{Na}_3\text{Fe}_3(\text{PO}_4)_4$ demonstrating excellent capacity retention at 10C for 6000 cycles.

References:

- 1) Bin, D. *et al.* Progress in aqueous rechargeable sodium-ion batteries. *Adv. Energy Mater.* **8**, 1703008 (2018).
- 2) Delmas, C. *et al.* Study of a layered iron (III) phosphate phase $\text{Na}_3\text{Fe}_3(\text{PO}_4)_4$ used as positive electrode in lithium batteries. *J. Electrochem. Soc.* **157**, A947 (2010).

September 9, 2021 (Thursday) 8:55-9:10

Characterization and Surface Deformation Behavior of Cu/Nb Nano Layered Composites

Mayur Pole^a, Tanvi Ajantiwalay^a, Shalini Tripathi^a, Hardeep Mehta^a, Tianhao Wang^a, Arun Devaraj^a, Bharat Gwalani^a

^a Pacific Northwest National Laboratory, Richland, Washington-99354

Presenter: Mayur Pole

Cu and Nb have negligible mutual solubility in the solid state. Recently, Cu-Nb thin films synthesized by various processing methods, such as, physical vapor deposition, and chemical vapor deposition showed promising mechanical and electrical properties at both ambient and elevated temperatures. This makes Cu-Nb promising for high mechanically stressed electrical and structural applications. Cu-Nb multi-layered nano laminates were synthesized by sputtering and their nano-mechanical properties, wear resistance and interfacial shearing between Cu and Nb was investigated in this study. Further, the effect of post annealing on the film's hardness, modulus, coefficient of friction wear mechanisms and the sub-surface shear deformation was studied. Transmission electron microscopy showed the increase in the grain size and a reduction in twin density in the Cu phase in the post annealing condition, which in turn lead to a reduction in the

hardness. The trends in wear resistance were opposite to that of hardness (deviating Archard's Law) and micro mechanisms responsible for this anomaly will also be discussed in the talk.

September 9, 2021 (Thursday) 9:10-9:25

Quantitative Measure of 3D Nanostructure and Size Dispersity of Ultrasmall Fluorescent Silica Nanorings via Small-Angle X-ray Scattering

Alvin Chang¹, Melik Turker^{1,2}, Paxton Thedford³, Ulrich Wiesner¹

¹Department of Materials Science and Engineering, Cornell University

²Elucida Oncology Inc., New York, New York 10016, United States

³Department of Chemistry and Chemical Biology and School of Chemical and Biomolecular Engineering, Cornell University

Ultrasmall nanoparticles have been receiving a growing amount of interest in several fields such as medicine, optics, and catalysis due to their unique size-dependent properties. Among these are fluorescent core-shell silica nanoparticles known as Cornell dots (or C dots), whose makeup is composed of a silica core and a poly(ethylene glycol) (PEG) shell [1]. These C' dots are poised to become promising diagnostic and therapeutic tools in medicine, in particular for applications in cancer. While regular spherical C dots have already been employed in FDA approved human clinical trials, exploration has expanded into different topologies of silica nanoparticles such as rings and cages [2], which boast a higher aspect ratio and also higher surface area to volume ratios and multiple different surfaces (*i.e.* inside versus outside). These features open the door towards orthogonal functionalizations of inside versus outside, as well as increased drug payloads, offering additional advantages relative to their spherical counterparts in therapeutics for nanomedicine. Past experiments have verified successful synthesis and characterization of orthogonally functionalized inner and/or outer surfaces of silica nanorings known as C rings [3]. However, quantitative assessments of size and size dispersity of such nanostructures remain parameters for further investigation. Many nanoparticle synthesis methods suffer from dispersity and/or aggregation problems, which is a critical issue especially in the case of ultrasmall nanoparticles designed to be renally cleared from the body, which has a cutoff below 10 nm. A quantitative determination of size distribution is therefore critical towards understanding and evaluating the effectiveness and safety of these nanorings in nanomedicine applications.

For the present study, particles were synthesized via a micelle template method in which mesitylene (TMB) swollen cetrimonium bromide (CTAB) micelles acted as a template for ~2 nm silica nanoclusters to form a ring-like shape around [2]. After forming the nanoring, the outer and inner surfaces of the rings were functionalized with deferoxamine (DFO) chelator (for radiolabeling) and were PEGylated with 6EO-PEG-silane on the outside and with 3EO-PEG-silane on the inside. To characterize 3D nanostructural details as well as their size and size dispersity, solution small-angle X-ray scattering (SAXS) was employed. SAXS, with the advantages of facile sample preparation, non-destructive measurements, and the ability to measure noncrystalline samples, is widely used in nanoparticle characterization. All SAXS measurements were performed at the Cornell High Energy Synchrotron Source (CHESS).

To determine the shape and 3D structure of C rings, various form factors such as the spherical shell, pearl necklace, raspberry, hollow cylinder, and torus were employed to analyze the

SAXS intensity profiles. All form factors except for the torus were modeled in the SASView software [4]. The torus model was implemented using the SASfit software [5]. The analysis using these models revealed that both the hollow cylinder and the torus models provide good quality fits of the experimental scattering intensity from the rings. It could further be shown that the scattering curve becomes nearly identical for the structural model of a hollow cylinder and a torus form factor with the same volume [6]. The hollow cylinder model had an inner radius of 2.8 nm with a polydispersity of 0.41, a cylinder thickness of 2.1 nm, and a cylinder length of 8 nm, which agrees well with the results of fluorescence correlation spectroscopy (FCS), indicating an 8.3 nm hydrodynamic size. SAXS analysis suggests multiple layers of silica nanoclusters averaging 2.1 nm assembled around the TMB/CTAB micelle to form an ultrasmall silica ring smaller than 10 nm.

In summary, we have analysed the 3D nanostructure of ultrasmall fluorescent silica nanorings using synchrotron based solution-SAXS experiments and their quantitative modeling. Future steps include analyzing silica nanorings with different radius and lengths by varying the silica, CTAB, and TMB ratios during synthesis.

References:

- [1] K.P. Barteau, *et al.*, Quantitative Measure of the Size Dispersity in Ultrasmall Fluorescent Organic-Inorganic Hybrid Core-Shell Silica Nanoparticles by Small-Angle X-ray Scattering, *Chem. Mater.* 2019, 31, 643-657.
- [2] K. Ma, *et al.*, Early Formation Pathways of Surfactant Micelle Directed Ultrasmall Silica Ring and Cage Structures, *J. Am. Chem. Soc.*, 2018, 140, 17343-17348.
- [3] M.Z. Turker, *et al.*, Inner and Outer Surface Functionalization of Ultrasmall Fluorescent Silica Nanorings As Shown by – High-Performance Liquid Chromatography, *Chem. Mater.* 2019, 31, 5519-5528.
- [4] <http://www.sasview.org/>.
- [5] Ingo Breßler, Joachim Kohlbrecher, and Andreas F. Thünemann, SASfit: a tool for small-angle scattering data analysis using a library of analytical expressions, *J Appl Crystallogr.* 2015 Oct 1; 48(Pt 5): 1587–1598.
- [6] S. Förster, *et al.*, Fusion of Charged Block Copolymer Micelles into Toroid Networks, *J. Phys. Chem. B* 1999, 103, 6657-6668.

September 9, 2021 (Thursday) 9:25-9:40

In situ AFM Study of Electrochemical Corrosion in FeCrNi Alloy in Deuterium Chloride Solution

Cheng-Han Li¹, Tingkun Liu¹, Jinhua Tao¹, and Arun Devaraj¹

Corresponding Author: arun.devaraj@pnnl.gov

¹. Physical and Computational Sciences Directorate, Pacific Northwest National Laboratory

Fe-Cr-Ni-based austenitic stainless steels have been widely used in marine and nuclear applications owing to their outstanding mechanical properties and corrosion resistance. Understanding the corrosion behavior especially in chloride-rich environment and effects of electrochemical reactions at the atomic scales is critical to develop advanced alloys with better corrosion resistance under extreme conditions [1, 2]. In this study, a combination of in situ atomic force microscopy (AFM) and ex situ transmission electron microscopy (TEM) was used to study the corrosion kinetics and microstructure evolution in a model Fe-18Cr-14Ni alloy using deuterium chloride (DCl + D₂O) with and without biasing.

References:

1. Pistorius, P.C. and G.T. Burstein, *Growth of corrosion pits on stainless steel in chloride solution containing dilute sulphate*. Corrosion Science, 1992. **33**(12): p. 1885-1897.
2. Ernst, P. and R.C. Newman, *Pit growth studies in stainless steel foils. I. Introduction and pit growth kinetics*. Corrosion Science, 2002. **44**(5): p. 927-941.

September 9, 2021 (Thursday) 9:40-9:55

Additive Manufacturing of Nanostructured Tungsten Coatings for Solar-Thermal Applications

V. Vinay K. Doddapaneni¹, Kijoon Lee², Tyler T. Colbert¹, Saereh Mirzababaei², Brian K. Paul², Somayeh Pasebani² and Chih-Hung Chang^{1,*}

¹. School of Chemical, Biological, and Environmental Engineering, Oregon State University, Corvallis, OR, U.S.A., 97331.

². School of Mechanical, Industrial, and Manufacturing Engineering, Oregon State University, Corvallis, OR, U.S.A., 97331.

W, a refractory metal with remarkable properties such as high strength, wear resistance, inherent IR reflectivity, has found its way to diverse applications. One growing use of W is as an absorber/IR reflective material for solar thermal applications. In this work, the feasibility of a new solution-processed method to manufacture nanostructured W coatings and their solar absorptance was investigated. A volatile precursor was deposited on Inconel 625 substrate and converted using a laser, simulating a selective laser melting process in a canister in an inert environment. W (BCC) was formed during laser-induced reaction in one step without further heat treatment. The solar absorptance varied from 63% - 97% depending on the amount of precursor deposited and oxygen content in the canister. With the growth of new hybrid additive manufacturing methods, this new solution-processed method will open avenues to manufacture W-based alloys, functional gradient materials, and coatings for high-temperature applications.

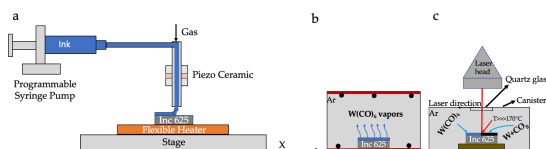


Figure 1 (a) Aerosol jet printing set up. **(b)** sublimation in a conventional furnace. **(c)** conversion in laser canister.

References:

[1] Gao, X.H., *et al.* Enhanced absorptance of surface-textured tungsten thin film for solar absorber. *Surf. Eng.* **2016**, 32, 840–845.

[2] Paul, B.K., *et al.* Oxide dispersion strengthened 304 L stainless steel produced by ink jetting and laser powder bed fusion. *CIRP Ann.* **2020**, 69, 193–196.

September 9, 2021 (Thursday) 9:55-10:30

Break

Session 4: Growth and Characterizations II. Chair: Tiffany Kaspar

September 9, 2021 (Thursday) 10:30-11:10

Strong correlations and topology in graphene-based moiré quantum materials (Invited)

Matthew Yankowitz^{1,2}

Corresponding Author: myank@uw.edu

¹. Department of Physics, University of Washington, Seattle, WA, USA

². Department of Materials Science and Engineering, University of Washington, Seattle, WA, USA

A wide family of atomically-thin van der Waals (vdW) materials can be mixed-and-matched to form heterostructures free of the typical interfacial lattice-matching constraints of epitaxial crystal growth, providing a simple path towards realizing on-demand designer electronics. The twist angle between neighboring crystals acts as a fundamentally new degree of freedom in these structures, controlling an emergent moiré superlattice potential that modifies the electronic band structure and overall device properties. In van der Waals heterostructures composed of two rotated graphene sheets, the moiré pattern creates very flat electronic bands over a small range of twist angles. A variety of highly tunable correlated and topological states have recently been identified in these platforms owing to the quenched kinetic energy of charge carriers and the intrinsic Berry curvature of the flat bands. I will survey our recent work investigating these states in three different twisted graphene platforms: twisted bilayer graphene (two rotated monolayer graphene sheets) [1], twisted double bilayer graphene (two rotated sheets of Bernal-stacked bilayer graphene) [2], and twisted monolayer-bilayer graphene [3-4]. We observe an array of correlated insulating states, superconductivity, orbital ferromagnetism, and topological Chern insulating states within these devices. These states can be controlled using experimental tuning knobs including the twist angle, charge doping, electric field, magnetic field, and pressure.

References:

- [1] M. Yankowitz, S. Chen, H. Polshyn, Y. Zhang, K. Watanabe, T. Taniguchi, D. Graf, A. F. Young, and C. R. Dean, Tuning superconductivity in twisted bilayer graphene, *Science* 363 (2019), 1059-1064.
- [2] M. He, Y. Li, J. Cai, Y. Liu, K. Watanabe, T. Taniguchi, X. Xu, M. Yankowitz, Symmetry breaking in twisted double bilayer graphene, *Nature Physics* 17 (2021), 26-30.
- [3] S. Chen, M. He, Y. Zhang, V. Hsieh, Z. Fei, K. Watanabe, T. Taniguchi, D. H. Cobden, X. Xu, C. R. Dean, M. Yankowitz, Electrically tunable correlated and topological states in twisted monolayer-bilayer graphene, *Nature Physics* 17 (2021), 374-380.
- [4] M. He, Y. Zhang, Y. Li, Z. Fei, K. Watanabe, T. Taniguchi, X. Xu, M. Yankowitz, Competing correlated states and abundant orbital magnetism in twisted monolayer-bilayer graphene, *Nature Communications* 12 (2021), 4724.

September 9, 2021 (Thursday) 11:10-11:25

Oxygen Vacancy Induced Polymorphs Formation in RF Sputtered TiO₂ and Widening of Stability Window of Low Temperature Polymorph

Pritha Biswas¹, Okan Agirseven¹, and Janet Tate¹

Corresponding Author: tate@physics.oregonstate.edu

¹Department of Physics, Oregon State University, Corvallis, OR 97331, USA

Stabilization of metastable polymorphs of TiO₂ is desired to achieve the different applications ranging from photocatalytic activity to gas sensors. We have previously reported that variations of the partial pressure of oxygen can stabilize high purity thin film of different polymorphs of TiO₂ including brookite in an RF sputter system.^[1] In this report, the interplay between oxygen partial pressure and polymorph stabilization is examined by in-situ Raman spectroscopy, and a plausible growth mechanism is established via Johnson-Mehl-Avrami-Kolmogorov (JMAK) analysis. All the previous literature indicates that Rutile should be thermodynamically most stable product and the trend of activation energy should be $\Delta G_{b, \text{Anatase}} < \Delta G_{b, \text{Brookite}} < \Delta G_{b, \text{Rutile}}$. Whereas an investigation of JMAK analysis on the nucleation rate and the activation energy of the polymorphs originated by this sputter deposited method indicates that there is a minimal difference in the energy offset of amorphous to crystalline transformation for three different polymorphs ($\Delta G_{b, \text{Anatase}} \approx \Delta G_{b, \text{Brookite}} \approx \Delta G_{b, \text{Rutile}}$). This modulation in activation energy of amorphous to the crystalline transition is happening due to two associated events, (i) Oxygen vacancy induced TiO₆ octahedral tilting and subsequent change in ratio of the edge share to corner share octahedra and (ii) the lower valence Ti³⁺ (self-dopant) induced modulation of growth kinetics. Moreover, it was found self-doping induced growth modulation results in enormous widening (400°C to 900°C) of the stability window of low temperature stable^[2] anatase TiO₂ without destroying the phase purity. Another metastable polymorph, brookite TiO₂ was also stabilized up to 700°C which may be of great importance in Lithium-ion battery, photocatalytic activity to high temperature gas sensing.

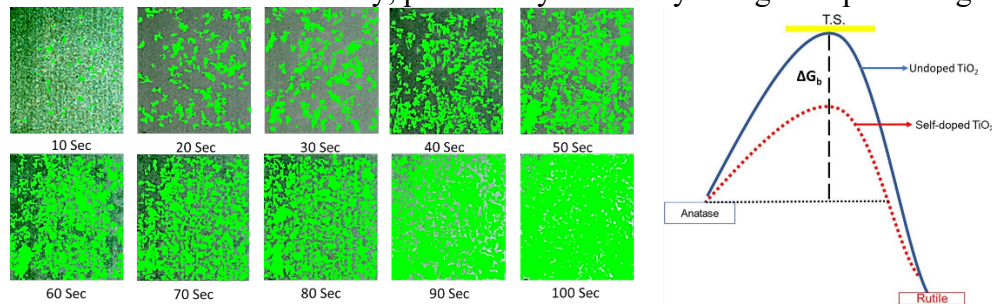


Figure 1 (a) Growth study of metastable brookite TiO₂ by In-situ Raman microscopy and effect of self-doping in energy offset.

References:

- [1] O. Agirseven, D. T. Rivella, Jr., J. E. S. Haggerty, P. O. Berry, K. Diffendaffer, A. Patterson, J. Krebs, J. S. Mangum, B. P. Gorman, J. D. Perkins, B. R. Chen, L. T. Schelhas, and J. Tate, Crystallization of TiO₂ polymorphs from RF-sputtered, amorphous thin-film precursors, *AIP Advances* 10 (2020), 0251091-0251097
- [2] H. M. Albetran, B. H. O'Connor, I. M. Low, Effect of pressure on TiO₂ crystallization kinetics using in-situ high-temperature synchrotron radiation diffraction, *Journal of American Ceramic Society* 100 (2017), 3199–320.

September 9, 2021 (Thursday) 11:25-11:40

Tensile-strained InGaAs quantum dots on GaSb(111)A via molecular beam epitaxy

Kevin D. Vallejo,¹ Trent A. Garrett,¹ Carlos I. Cabrera-Perdomo,² Madison D. Drake,¹ Baolai Liang,³ Kevin A. Grossklaus,⁴ and Paul J. Simmonds^{1, 5,a)}

Corresponding Author: paulsimmonds@boisestate.edu

1) Micron School of Materials Science & Engineering, Boise State University, Boise, ID 83725, USA. 2) Center for Research in Sciences, Research Institute in Basic and Applied Sciences, Autonomous University of the State of Morelos, Av. Universidad 1001, 62209, Cuernavaca, Morelos, Mexico 3) California NanoSystems Institute, University of California Los Angeles, CA 90095, USA. 4) Department of Electrical and Computer Engineering, Tufts University, Medford, MA 02155 USA 5) Department of Physics, Boise State University, Boise, ID 83725, USA.

We have determined a reproducible set of growth conditions for the self-assembly of tensile-strained In_{1-x}Ga_xAs quantum dot nanostructures on GaSb(111)A surfaces. During molecular beam epitaxy, In_{1-x}Ga_xAs islands form spontaneously on GaSb(111)A when the Ga content $x \geq 50\%$. We demonstrate control over the size and areal density of the islands as a function of deposition amount, V/III BEP ratio, and substrate temperature. We analyzed the samples with InGaAs layers on GaSb(111)A using atomic force microscopy (AFM), reflection high-energy electron diffraction (RHEED) and compare morphological attributes with similarly grown In_{1-x}Ga_xAs islands on InAs(111)A substrates. This work demonstrates previous efforts to establish (111)-oriented

materials from the 6.1 Å family of semiconductors as new platforms for device research based on optimized InAs(111) epitaxy [1] and strain-driven quantum dot technologies [2].

References: [1] K. D. Vallejo, T. A. Garrett, K. E. Sautter, K. Saythavy, B. Liang, and P. J. Simmonds, “InAs(111)A homoepitaxy with molecular beam epitaxy,” *Journal of Vacuum Science & Technology B*, 37, 061810 (2019) [2] K. D. Vallejo, K. E. Sautter, and P. J. Simmonds, “Strain-driven quantum dot self-assembly by molecular beam epitaxy,” *Journal of Applied Physics* 128, 031101 (2020).

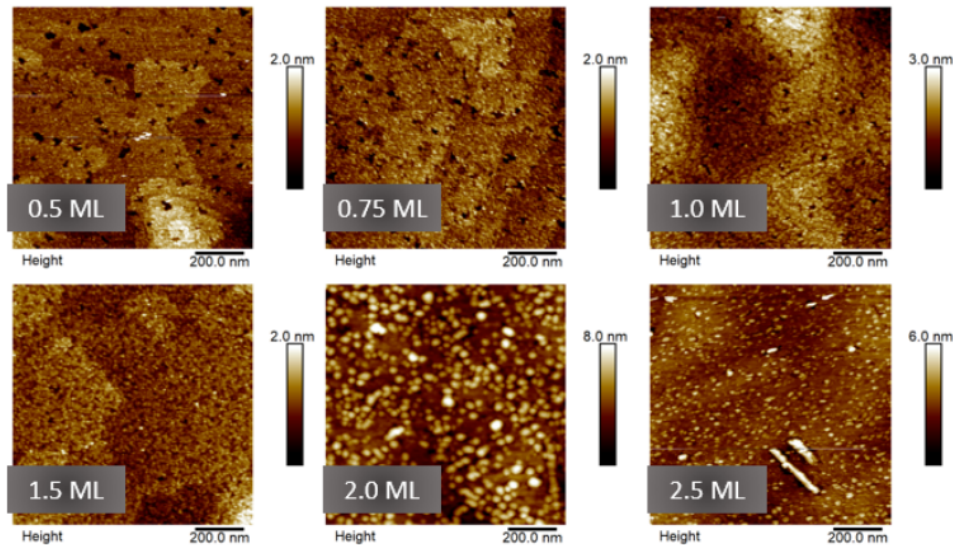


Figure 1 1 μm x 1 μm scans taken using atomic force microscopy of the surface of In_{0.5}Ga_{0.5}As QDs grown with various thicknesses. We grew this series at a T_{sub}= 420°C and a growth rate of 0.4 ML/s.

September 9, 2021 (Thursday) 11:40-11:55

Decoupling of Strain and Temperature Effects on Microstructural Evolution during High Shear Strain Deformation

Anqi Yu,^{1,2} Mayur Pole,^{1,3} Julian D Escobar Atehortua,¹ Krassimir Bozhilov,² Jia Liu,¹ Joshua A Silverstein,¹ Sundeep Mukherjee,³ Suveen Mathaudhu,^{1,2,4} Arun Devaraj,¹ Bharat Gwalani¹

Corresponding Author: anqi.yu@pnnl.gov

1Physical and Computational Sciences Directorate, Pacific Northwest National Laboratory, Richland, WA, 99352, USA

2Material Science and Engineering Program, University of California, Riverside, Riverside, CA, 92521, USA

3Materials Science and Engineering Department, University of North Texas, Denton, Texas, 76207, USA

4Metallurgical and Materials Engineering Department, Colorado School of Mines, Golden, CO, 80401, USA

The interplay between defect generation by shear strain and defect annihilation by local heating is difficult to predict in shear assisted processing techniques. In this study we decoupled the effects of high shear strain and external heating in an immiscible Cu-Nb alloy using a pin-on-disk tribometer to mimic the microstructural evolution of material during solid phase processing. The change in sub-surface deformation, strain distribution and redistribution of second phase as a function of temperature were examined using transmission electron microscopy and atom probe tomography. Comparison with a bulk scale process were made by quantifying the deformation using Zener Holloman parameter.

September 9, 2021 (Thursday) 11:55-12:10

Nucleation and growth of molybdenum disulfide grown by thermal atomic layer deposition on metal oxides

Jake Soares¹, Steven Letourneau^{1,2}, Matthew Lawson¹, Anil U. Mane², Jeffrey W. Elam², and Elton Graugnard¹

Corresponding Author: eltongraugnard@boisestate.edu

¹ Boise State University, Micron School of Material Science and Engineering, 1910 University Dr., Boise, ID 83725, USA

² Argonne National Laboratory, Energy Systems Division, 9700 S Cass Ave, Lemont, IL 60439, US

To enable greater control over the thermal atomic layer deposition (ALD) of molybdenum disulfide (MoS₂), here we report studies of the reactions of molybdenum hexafluoride (MoF₆) and hydrogen sulfide (H₂S) with oxide substrates from nucleation to few-layer films. The first ALD half cycle was investigated to gain insight into initial bonding and byproduct formation. These results supported the creation of metal-fluoride species and MoO_x bonds. Density functional theory, coupled with free energy calculations, helped determine reaction equations for the first half cycle. Following early nucleation stages, the transition to steady growth was investigated. In-situ quartz crystal microbalance measurements and Fourier transform infrared absorbance spectra were used to determine that Mo-S bonds start to form after roughly nine cycles. X-ray photoelectron spectroscopy of as-deposited films indicate a large presence of MoO_x bonding with low concentrations of MoS₂. Studies of nucleation and steady growth help influence post deposition processing. Annealing of films in a high temperature H₂S environment provides thermal energy for crystallization of MoS₂ films. Few layer MoS₂ films were deposited and verified by Raman spectroscopy and transmission electron microscopy. Additional processing was investigated showing increased annealing temperatures led to better crystallinity in few layer films. This work helps further the understanding of 2D MoS₂ deposition and supports the integration of 2D TMDCs into semiconductor manufacturing.

September 9, 2021 (Thursday) 12:10-12:25

Determining the Adsorption Mechanism of 2,3-butanediol on RuO₂ using First Principles Calculations Coupled with Global Optimizers

Carrington Moore¹, Difan Zhang², Roger Rousseau², Vassiliki Alexandra Glezakou², Jean-Sabin McEwen¹

Corresponding Authors: vanda.glezakou@pnnl.gov, Roger.Rousseau@pnnl.gov,

js.mcewen@wsu.edu

¹. Gene and Linda Voiland School of Chemical Engineering and Bioengineering, Washington State University Pullman, WA, United States of America

². Physical and Computational Sciences Directorate, Pacific Northwest National Laboratory, Richland, WA 99352, United States of America

2,3-butanediol has been identified as a potential source to produce butene, because of its sustainability as a biomass-derived sugar. While studies have explored the conversion of 2,3-butanediol to butene, little is understood about the mechanistic details of this reaction. As a first step toward this goal, we modeled its reaction mechanism in the absence of a catalyst as well as its adsorption on RuO₂(110). The differential charge analyses regarding the adsorption 2,3-butanediol (Figure 1A-C) demonstrate that having the oxygen functional groups of 2,3-butanediol point toward the surface of RuO₂(110) will result in forming a new strong chemical bond.

The ruthenium atoms act as Lewis acid sites by bonding with the oxygen functional groups of 2,3-butanediol, whereas lattice oxygen species act as Lewis bases. The most favorable adsorption configuration of 2,3-butanediol was tested initially by chemical intuition and then later compared with the results from the NWPEsSe global optimizer. The strong similarity between the two ground state structures (Figure D, E) indicates that the stronger adsorption energy in the NWPEsSe-derived structure is related to the adsorption configuration of the adsorbate. The dehydration reaction could require a stronger adsorption energy that would necessitate surface defects such as oxygen vacancies, and, as the global optimizer has been proven to provide accurate adsorption energies, it will provide a more comprehensive analysis for the more complex adsorbates in the presence of surface defects.

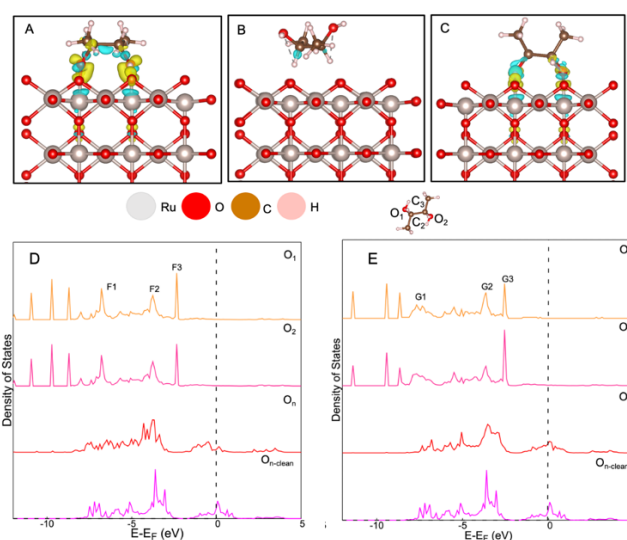


Figure 1. Charge differential analysis for the adsorption of 2,3-butanediol on RuO₂(110) (A-C), the corresponding partial density of states analysis (D-E).

September 9, 2021 (Thursday) Afternoon

Plenary Session (II): Chair: Xiao-Ying Yu

September 9, 2021 (Thursday) 12:40-13:30

**In-situ/operando soft x-ray spectroscopy of chemical and catalytic interfaces
(Plenary)**

Jinghua Guo¹

¹. Lawrence Berkeley National Laboratory, Berkeley, CA, United States of America

The energy materials and devices have been largely limited in a framework of thermodynamic and kinetic concepts or atomic and nanoscale. Soft x-ray spectroscopy characterization offers unique characterization in many important energy materials of energy conversion, energy storage and catalysis in regards to the functionality, complexity of material architecture, chemistry and interactions among constituents within.

It has been found that the microstructure and composition of materials as well as the microstructure have a great influence on performances of energy conversion and energy storage materials, chemical and catalytic processes. However, it is challenging to reveal the real mechanism of the chemical processes. In-situ/operando x-ray spectra characterization technique offers an opportunity to uncover the phase conversion, chemical speciation at the solid/gas and solid/liquid interfaces in real time.

I will give some basics on in situ/operando soft x-ray spectroscopy characterization of interfacial phenomena in energy materials and devices, and how to use the powerful in-situ/operando characterization techniques, e.g. soft x-ray absorption spectroscopy (XAS) and resonant inelastic soft x-ray scattering (RIXS) to investigate the real electrochemical mechanism during the operation. A number of electrochemical liquid cells will be presented with success in revealing the catalytic and electrochemical reaction at real time.

Session 5: Biology and Environmental Study I. Chair: Xiao-Ying Yu

September 9, 2021 (Thursday) 13:30-14:10

Microbial Phenotype Probed by Mass Spectrometry: From Bottom Up Proteomics to Metabolite Imaging (Invited)

Luke Hanley, LAS Distinguished Professor
Department of Chemistry
University of Illinois Chicago
chem.uic.edu/profiles/luke-hanley or →



Pseudomonas aeruginosa is a problematic opportunistic pathogen often isolated from burn wounds, pressure ulcers and cystic fibrosis patient lungs. Proteomics can help elucidate different metabolic strategies utilized by this pathogen when grown as either planktonic or biofilm cultures. The role of carbon, nitrogen and energy sources such as glucose, lactate, and amino acid nutrients are of interest as they contribute to cellular growth, maintenance, and structural support. Several strategies in mass spectrometry are described here that probe the phenotype of a clinical isolate of *P. aeruginosa* grown both planktonically and as biofilms in amino-acid rich, lactate-enriched media.

Untargeted label free quantification, bottom up proteomics were applied to illuminate metabolic differences in a comparative analysis of planktonic cultures and sessile membrane biofilms of *P. aeruginosa* [1]. Liquid chromatography electrospray ionization tandem mass spectrometry (LC-

MS-MS) was performed on a Thermo Fisher Scientific Orbitrap Velos Pro, MaxQuant software was used for protein identification and label-free quantification, statistical analysis was performed by Perseus software, and functional enrichment analyses were performed with the String database search engine. Preferential use of different substrates was observed based on protein abundance changes, suggesting shifts in metabolic strategies as a function of nutrient environment.

The aforementioned work required sampling of multiple entire biofilms which thereby averaged over a range of phenotypes within each biofilm [1]. Laser ablation sample transfer (LAST) was therefore used for site-specific sampling which, when combined with bottom up proteomics, was able to distinguish radially and axially resolved proteomes for *P. aeruginosa* biofilms [2]. Specifically, differential protein abundances were observed on aerobic vs. anaerobic regions of a biofilm with higher sensitivity than previously observed [1]. LAST also allowed spatially resolved analysis of metabolites within intact biofilms [2].

Liquid chromatography and proton nuclear magnetic resonance were used to delineate changes in the metabolome [1]. However, these methods are limited in sensitivity, chemical selectivity, and their ability to reveal spatial distributions within biofilms. An alternative to secondary ion mass spectrometry is under development for probing metabolites in biofilms: femtosecond laser desorption postionization mass spectrometry imaging can to probe biofilms with micron-scale resolution [3-5]. This new method in mass spectrometry imaging will be combined with established genomic and proteomic strategies to refine computation metabolic models that reflect the chemical complexity associated with microbial phenotype.

[1] Y.P. Yung, S.L. McGill, H. Chen, H. Park, R.P. Carlson, and L. Hanley, *npj Biofilms and Microbiomes* **5** (2019) 31. <https://rdcu.be/b82cd>

[2] A.C. Pulukkody, Y.P. Yung, F. Donnarumma, K.K. Murray, R.P. Carlson, and L. Hanley, *PLOS ONE* **16**:7 (2021) e0250911 and references therein. <https://doi.org/10.1371/journal.pone.0250911>

[3] L. Hanley, R. Wickramasinghe, and Y.P. Yung, *Annu. Rev. Anal. Chem.* **12** (2019) 225. <https://doi.org/10.1146/annurev-anchem-061318-115447>

[4] *Photoionization and Photo-induced Processes in Mass Spectrometry: Fundamentals and Applications*, R. Zimmermann and L. Hanley, editors, (2021) Wiley-VCH, Berlin, ISBN: 978-3-527-35510-7.

[5] C.L. Pieterse, I. Rungger, I.S. Gilmore, R.C. Wickramasinghe and L. Hanley, *J. Phys. Chem. Lett.* **11** (2020) 8616. <http://dx.doi.org/10.1021/acs.jpcllett.0c02365>

Poster Session at Gather.Town:
September 9, 2021 (Thursday) 14:10-15:30

Poster 1. Understanding the Role of Aliovalent Al Doping at the Mg Metal Battery Interface using *Operando* and *In-situ* Spectroscopy

Luke Soule^{1,2}, Venkateshkumar Prabhakaran^{1,2}, Grant E. Johnson^{1,2}, Jaegeon Ryu^{1,2}, Sungun Wi^{1,2}, Vaithiyalingam Shutthanandan¹, Karl T. Mueller^{1,2}, and Vijay Murugesan^{1,2},

¹Pacific Northwest National Laboratory, Richland, Washington 99352, United States.

²Joint Center for Energy Storage Research (JCESR), Lemont, Illinois 60439, United States.

A molecular-level understanding of the surface chemistry occurring at electrode-electrolyte interfaces (EIs) during charge transfer processes is necessary to enable the rational design of efficient “beyond-Li ion” energy storage technologies such as Mg-ion batteries. The reversible plating and stripping of Mg²⁺ cations on Mg metal anodes are often accompanied by inefficiencies due to electrolyte decomposition, as well as poor mass- and charge-transport at the solid-electrolyte interphase (SEI) layers. These limitations affect device-level performance and stability. In this work, we studied the effect of aliovalent dopant Al nanoclusters on controlling the charge and mass transfer of Mg²⁺ ions during Mg plating and stripping processes at interfaces. We developed a unique multimodal characterization platform that combines controlled deposition of ions and metal clusters (soft- and hard-landing) with *in-situ* electrochemical impedance spectroscopy (EIS), *operando* Raman spectroscopy, and *in-situ* x-ray photoelectron spectroscopy (XPS). Our multimodal platform enabled us to: (i) prepare well-defined electrode interfaces containing specific species of interest; (ii) study the effect of aliovalent doping with Al on mitigating the degradation of electrolyte species during the Mg plating and stripping processes. A significant change in the overpotential and charge transfer resistance for plating and stripping in the presence of Al doping is revealed by *in-situ* EIS, whereas *operando* Raman and *in-situ* XPS were used to characterize the changes in the structural and chemical state of the SEI layers. In this presentation, we will describe how our multimodal platform enabled us to determine the role of Al clusters at the SEI in modulating interfacial charge transfer kinetics and chemical degradation at Mg battery interfaces.

Keywords: Mg battery, solid-electrolyte interphase, operando spectroscopy

Poster 2. Characterization and Confirmation of Products of Zeolitic Imidazolate Framework 8 (ZIF-8) Thin-Film, Room-Temperature, Microfluidic Pen Synthesis

Hsin-Mei Kao, Yujing Zhang, Victoria Chang, Vinay Doddapaneni, and Chih-Hung Chang
Cole DeCesare: decesarc@oregonstate.edu

School of Chemical, Biological and Environmental Engineering, Oregon State University, Corvallis OR, USA.

Zeolitic imidazolate framework-8 (ZIF-8) is a nanoporous metal-organic framework (MOF) material that can be synthesized in an aqueous or alcoholic solvent. ZIF-8 has many potential applications such as catalysis, gas capture, drug delivery, sensors, and more.^[1]

Recent studies on patterned MOF thin films have been a vibrant research field for emergent industrial applications such as optoelectronics and smart coatings. The motivation behind this project is to print ZIF-8 using lesser reagents and reduced waste, which can lead to lower production costs and ensure its capability for desired applications. Microfluidic devices take advantage of the physical and chemical properties of liquids at the microscale, allowing for less chemical volume and, therefore, lower cost while also shortening experiment time. Using vMFP, MOF precursors can be confined through a reactor (i.e., the vMFP head) and onto a substrate, reducing the reaction time for MOF thin film synthesis while increasing the yield. Attaching the vMFP to a pen-plotting device allows for the precise control of deposition, allowing for patterns and designs to be created with the MOF thin film, extending applications of the MOFs. Batch and continuous flow synthesis were carried out using a vertical MicroFluidic Probe (vMFP).^[2]

Analysis of XRD patterns from ZIF-8 coated substrates using aqueous-based chemistry show peaks differ from ZIF-8. In contrast, using methanol as a solvent instead of water, ZIF-8 was successfully produced. Future experimentation with different reactant molar ratios, reaction time and temperature, and improved pen head designs will be conducted.

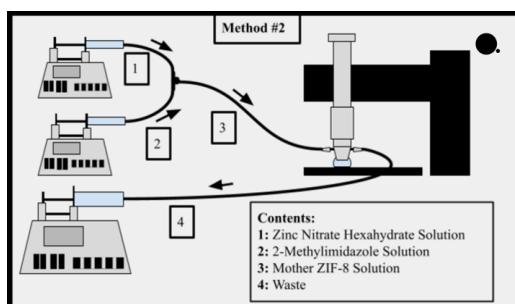


Figure 1 A depiction of the microfluidic pen ZIF-8 Synthesis^[2] method

References:

- [1] S. Fatemi, *et al.*, A comparative study on ZIF-8 synthesis in aqueous and methanolic solutions: Effect of temperature and ligand content, *Solid State Sciences* (2019), 108-112.
[2] Y. Zhang, *et al.*, *Metal-Organic Framework Thin Films: The Synthesis and The Application*, Oregon State University (2020), 1-222.

Poster 3. Controlling the Morphology of Vapor Phase Deposition of Tungsten by Different Heating Techniques

^{1,*} Beckett Lewis, V. Vinay K. Doddapaneni, Jeffrey Dhas, and Chih-Hung Chang

1. School of Chemical, Biological, and Environmental Engineering, Oregon State University, Corvallis, OR, U.S.A., 97331.

Chemical Vapor Deposition (CVD) is a widely utilized process for applying thin coatings onto substrates facilitated by chemical reactions. One of the significant advantages of CVD is its numerous applications in industry stemming from its highly adaptable methods and ability to be modified to accommodate a wide variety of precursors. This study used solid tungsten

hexacarbonyl as a precursor material to deposit tungsten from the vapor phase. Tungsten was chosen as the material for this study because of its desirable qualities, specifically its high melting point, good thermal and electrical conductivity, chemical stability, high hardness, and its growing applications in nuclear and solar-thermal fields. The methods used involved the sublimation of solid tungsten hexacarbonyl and then transport by an inert carrier gas onto a glass substrate. In the hotbed method (HBM), the glass substrate was maintained at the decomposition temperature of the precursor. In the cold bed method (CBM), the deposited precursor was converted using an IR laser. These two different heating techniques allowed control over the morphological structure of the deposits and can tune the properties of tungsten based on application. The samples were examined using X-Ray Diffraction and scanning electron microscopy (SEM).

References:

- [1] Creighton, J.R., *et al.* Introduction to Chemical Vapor Deposition (CVD). *ASM International*. **2001**, 3-7.
- [2] Wang, W., *et al.* Self-doped W-WO_x nanocermet multilayer films fabricated by single tungsten target reactive sputtering for selective solar absorption. *Journal of Materials Chemistry*. **2018**, 6, 15690-15700.
- [3] Klecka, J., *et al.* Tailoring the structure of RF-ICP tungsten coatings. *Surface and Coatings Technology*. **2021**, 406, 126745.

Poster 4. Inkjet Printed Europium-doped Yttria for Anti-Counterfeiting on Stainless Steel and Glass

Yujuan He^a, Jeffrey Dhas^a, Kijoon Lee^b, Milad Ghayoor^{b,c}, Somayeh Pasebani^{b,c}, Brian K. Paul^b, Chih-hung Chang^{a,*}

Corresponding author: chih-hung.chang@oregonstate.edu,

^a*School of Chemical, Biological and Environmental Engineering, Oregon State University, Corvallis, OR, USA.*

^b*School of Mechanical, Industrial and Manufacturing Engineering, Oregon State University, Corvallis, OR, USA.*

^c*Advanced Technology and Manufacturing Institute (ATAMI), Corvallis, OR, 97330, United States*

Anti-counterfeiting technologies are essential for advancements in product authentication processes and intellectual property protection. There has been an increasing demand in the aerospace, automotive, and medical industries to develop and integrate anti-counterfeiting technologies enabled by inorganic materials such as alloys, ceramics, and glasses. The following work demonstrates a facile and scalable approach to the multifunctional fabrication of anti-counterfeiting features. Through the use of low-cost precursor inks deposited via inkjet printing and subsequent decomposition via thermal conversion, Y₂O₃:Eu is successfully printed to fabricate anti-counterfeiting patterns on glass and stainless-steel substrates. Through variations in droplet spacing during inkjet printing, an invisible pattern is observed under normal light while exposure under ultraviolet light shows a distinct fluorescent pattern.

References:

- [1] C. Wei, Z. Sun, Y. Huang, L. Li, Embedding anti-counterfeiting features in metallic components via multiple material additive manufacturing, *Additive Manufacturing*. 24 (2018) 1–12. <https://doi.org/10.1016/j.addma.2018.09.003>.

[2] N. Gupta, F. Chen, N.G. Tsoutsos, M. Maniatakos, ObfusCADE: Obfuscating Additive Manufacturing CAD Models Against Counterfeiting: Invited, in: Proceedings of the 54th Annual Design Automation Conference 2017 on - DAC '17, ACM Press, Austin, TX, USA, 2017: pp. 1–6. <https://doi.org/10.1145/3061639.3079847>.

[3] F. Chen, G. Mac, N. Gupta, Security features embedded in computer aided design (CAD) solid models for additive manufacturing, *Materials & Design*. 128 (2017) 182–194. <https://doi.org/10.1016/j.matdes.2017.04.078>.

[4] Z.C. Kennedy, D.E. Stephenson, J.F. Christ, T.R. Pope, B.W. Arey, C.A. Barrett, M.G. Warner, Enhanced anti-counterfeiting measures for additive manufacturing: coupling lanthanide nanomaterial chemical signatures with blockchain technology, *J. Mater. Chem. C*. 5 (2017) 9570–9578. <https://doi.org/10.1039/C7TC03348F>.

[5] Murdock Charitable Trust, Department of Energy (DOE), RAPID, ATAMI

Poster 5. Reaction of 2-Propanol on SnO₂(101) Studied using Ambient-Pressure X-ray Photoelectron Spectroscopy

Jessica Jenkins, Radwan Elzein, Rafik Addou, and Gregory S. Herman

School of Chemical, Biological, and Environmental Engineering, Oregon State University, Corvallis, OR, 97331, USA

Abstract:

It has been shown the crystallographic planes of tin dioxide (SnO₂) play a critical role in the oxidation/reduction properties and the resulting surface chemistries. SnO₂ has been extensively studied due to its versatility in many areas of interest such as oxidation catalysis, transparent oxide conductors, and gas sensing. It has been recently demonstrated that the oxidation of volatile organic compounds (VOCs) is catalyzed by SnO₂, where 2-propanol was used as a representative VOC. In UHV, the transition from a stoichiometric to a reduced SnO₂(101) surface occurs at temperatures above 500 K, which is a higher temperature than observed for SnO₂(110). The dual valency of the Sn enables the reduction of the SnO₂ surface and a transition from the Sn⁺⁴ to the Sn⁺² oxidation state. Furthermore, recent studies indicate the ratio of Sn⁺²/Sn⁺⁴ on SnO₂ nanomaterials strongly impact the activity of the oxidation of carbon monoxide. For this study, we have utilized ambient pressure X-ray photoelectron spectroscopy (AP-XPS) and low energy electron diffraction (LEED) to characterize the surface chemistry of 2-propanol on well-defined SnO₂(101) surfaces. These results will be compared to similar studies performed on a SnO₂(110) surface. This allows a direct comparison of the catalytic properties and the electronic states of the two surface terminations. Further investigations using AP-XPS were done on the SnO₂(101) in the presence of 2-propanol up to 3 mbar at 380 K. By using valence-band spectra during reaction conditions we confirm the transition of Sn⁺⁴ to Sn⁺² in the presence of 2-propanol. The reaction selectivities will be compared for the various reaction conditions for SnO₂(101) and SnO₂(110) and will be related to the surface atomic structure.

Poster 6. Effects of Lattice Hydrogen Concentration on Ammonia Synthesis Over Palladium

Zachary Evans¹, and Líney Árnadóttir¹

Corresponding Author: liney.arnadottir@oregonstate.edu

¹. *School of Chemical, Biological and Environmental Engineering, Oregon State University, Corvallis, Oregon 97331, United States.*

Ammonia is a key ingredient in fertilizers and therefore critical to earth's food productions. Currently, the majority of ammonia synthesis is done with the Haber-Bosch process, developed in 1913, which is energy efficient but has a high carbon footprint. Electrochemical ammonia synthesis has also been proposed as a feasible alternative for distributed ammonia synthesis at low temperatures and pressures. One of the challenges to such implementation is the competition between the hydrogen evolution reactions (HER) and NH₃ synthesis in aqueous electrochemical systems. Identifying catalysts and/or conditions that could increase selectivity towards dinitrogen reduction over HER is an important step towards aqueous ammonia synthesis. Palladium is an intriguing catalyst for ammonia synthesis due to its ability to form a palladium hydride and subsequently provide a source of hydrogen for the reduction of nitrogen adsorbed on the metal surface. Here we study the effects of hydrogen content in the palladium lattice on the critical steps of HER and ammonia synthesis using density functional theory. Palladium hydride can affect the relative rate of these reactions in various manners, by providing a different source of hydrogen, as well as affecting initial and transition states of different elementary steps through differences in palladium hydride levels and/or changes in the lattice constants. How these effects change the onset potentials and relative rate of the different reactions can provide useful insights into how palladium hydride catalysts may be refined.

Poster 7. Continuous flow synthesized nanoparticles

Han Mei¹, and Chih-hung Chang¹

Corresponding Author: Chih-hung.Chang@oregonstate.edu

¹. *School of Chemical, Biological and Environmental Engineering, Oregon State University, Corvallis, Oregon 97331, United States.*

Colloidal semiconductor quantum dots exhibit a variety of size- and shape-dependent physical and chemical properties which offer a unique opportunity for us to make nanomaterials with tailored characteristics. Many studies have been applied on nanomaterials in solar cells, thin film transistors, chemical sensors, light-emitting diodes, and bio-imaging. Conventionally, hot injection is popular for synthesizing colloidal quantum dots (CQDs), due to its fast and controllable properties during synthesis. But many drawbacks have been found during the last decade when people try to commercialize the product, such as uncontrollable quenching process, unpredictable mixing rate, various heat transportation rates, and low throughput. The larger the reaction vessel, the harder the good size and shape control can be achieved. In these aspects, continuous flow exhibits extraordinary ability to control these factors. By spatiotemporal transformation, if the tubing size and the flowrate inside the tubing are fixed, the reaction will only rely on the length of the equipment. For the narrow tubing, mixing inside will be vigorously happened, and the heat-transfer path will be greatly reduced, which makes the reaction happen more efficiently. As well as separating seeding

and growth process, it offers us an opportunity to control the number of seeds in seeding stage, in principle, the more seed formation happens in the seeding stage, the smaller quantum dots can be obtained from reaction. With the same reaction rate and yielding, simply scaling up numbers of reaction tubing will result in high throughput reaction and more product.

Based the hot-injection method, a modified continuous flow reaction is designed with peristaltic pump. Lead precursor is preheated to some certain temperature and mixed with room temperat-

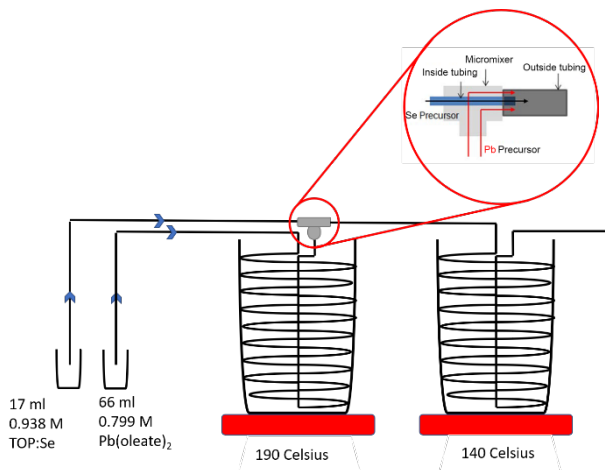


Figure 1. Experiment setup

ure selenium precursor. By adjusting seeding, growth temperature and residence time. Various sized Quantum dots could be achieved.

From 190 Celsius seeding, 140 Celsius growth, and 2 minutes reaction. TEM results exhibit

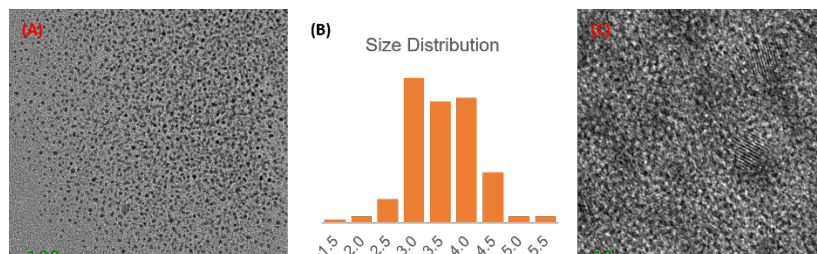


Figure 2. TEM results, with average size 3.29 nm and deviation 0.415 nm.

quantum dots in small size with a narrow size distribution. Those results give us a great inspiration to continue study on parameters optimization and high-production achievement.

Key words: Continuous flow, Various sized Quantum Dots

Poster 8. Understanding Cloud Condensation Activity of Aerosol with Higher Temporal Resolution

Abu Sayeed Md Shawon¹, Gouri har Kulkarni¹, and Swarup China¹

¹Pacific Northwest National Laboratory, Richland, Washington 99352, United States.

Every cloud droplet in Earth's atmosphere requires adequate relative humidity and a pre-existing aerosol particle in the atmosphere. A cloud droplet forms by condensing water the vapor on the aerosol that acts as a nucleus of that droplet. Aerosol particles that form droplets are called cloud

condensation nuclei (CCN). This interaction between aerosol and cloud is a parameter that prominently affects the earth's radiative budget through their warming and cooling effects, hydrological cycle through precipitation, and in a long term, climate. However, this interaction poses one of the largest uncertainties in climate modeling. Improvement of this scenario requires reliable instrumentation with high spatial and temporal resolution.

One of the reliable instruments that measure how readily an aerosol particle would form a cloud droplet is cloud condensation nuclei counter (CCN Counter). Traditionally, given the default instrumentation, a CCN Counter sets the relative humidity by creating a temperature gradient along its cylindrical volume. It maintains a constant pressure and flow rate during this process via its built-in pumps. Temperature stabilization being a slow process, this mode operation has a poor temporal resolution and a limited number of set humidity. During the airborne measurements and field campaigns where the meteorological conditions can change rapidly, this method cost valuable details of the CCN activity of aerosol. We significantly improved this resolution by altering some built-in instrumentation and developing a new method of operation where flow parameters varied instead of the temperature gradient. We also obtained a calibration curve showing relative humidity as a function of the flow parameters (on the contrary to the traditional relative humidity as a function of temperature gradient curve).

September 9, 2021 (Thursday) 15:30-16:00

Break

Session 6: Energy Applications I. Chair: Mark Engelhard

September 9, 2021 (Thursday) 16:00-16:40

Mapping the effects of physical and chemical reduction parameters on local atomic distributions within bimetallic nanocrystals (Invited)

Liane Moreau

Assistant Professor, WSU department of chemistry

Abstract: Bimetallic metal nanoparticles are of broad interest due to their unique optical and catalytic properties which provide hybrid characteristics in comparison to monometallic counterparts. Associated properties in AgAu particles have typically been attributed to the presence of Ag-Au bonds, which follow the assumption that miscibility favors homogeneous alloy formation. This assumption is problematic, in that thermodynamics does not necessarily favor Ag-Au mixing, and necessitates the atomic-scale characterization of synthesized particles in order to accurately correlate observed properties with atomic scale distributions of the separate metal species.

Presented work includes a systematic investigation of how the parameters that control metal ion reduction affect the atomic scale distribution of Ag and Au within bimetallic nanocrystals. Given the substantial differences in redox properties between these two metals, we explore the hypothesis that reduction kinetics can be applied to tune the atomic scale incorporation and distribution of Ag and Au within synthesized particles. In particular, the roles of Ag:Au atomic ratio, the ratio of reducing agent to metal and the volume of reducing agent introduced (low, concentrated volume vs. larger, dilute volume) will be discussed. The synthetic space is thoroughly investigated using electron microscopy (TEM) and small angle X-ray scattering (SAXS) to probe effects on particle morphology, X-ray fluorescence (XRF) to elucidate incorporation ratios of Ag vs. Au, X-ray absorption spectroscopy (XAFS) to map coordination environments and consider alloy homogeneity vs. clustering and UV-vis spectroscopy to consider how the aforementioned parameters affect the optical properties of the resulting constructs. Overall, we find that reduction parameters indeed contribute to the atomic scale distribution of species within bimetallic nanocrystals, leading to the proposal of ways in which such particles can best be optimized for use as optical sensors and catalytic substrates.

September 9, 2021 (Thursday) 16:40-16:55

Structure and Properties of Epitaxial LiCoO₂ thin films

Widitha Samarakoon^{1,2}, Zhenxing Feng¹, Le Wang², Jinhui Tao², and Yingge Du²

Corresponding Author: yingge.du@pnnl.gov

¹. School of Chemical, Biological and Environmental Engineering, Oregon State University, Corvallis, Oregon 97331, USA

LiCoO₂ (LCO) is the most widely studied and used cathode material in Li-ion batteries¹. Despite being commercialized for several decades, challenges such as capacity fading and voltage decay during high voltage cycling are brought about by aggravated degradations at the surface and the bulk². Epitaxial thin films, with well-defined atomically sharp interfaces, controlled orientation, free from additives, binders, and other impurities can be used as model systems to study intrinsic structure-property relationships³. In this work, we used pulsed laser deposition (PLD) to grow epitaxial thin films of LCO on (001), and (111)-oriented single crystalline SrTiO₃ (STO) substrates. Under the growth conditions, LCO formed unique types of defects, dictated by the substrate orientation, namely twin-boundaries in (001), and anti-phase boundaries in (111)-oriented STO. Furthermore, the type of defect present determined the orientation, and connectivity of Li⁺ containing planes, and diffusion channels thereby mediating the long-term structural stability of the cathode. To investigate the charge-discharge induced morphological, and structural changes and evolution of the cathode electrolyte interface (CEI), and phase transition layer (PTL) in real time, we conducted in situ electrochemical atomic force microscopy (EC-AFM) studies. We observed unique surface morphology evolution during de-intercalation, in each system, namely expansion of grains, and lattice gliding. The results from this study reveal structural and morphological origins behind different failure modes of LCO and provide insights into designing robust energy storage materials and devices.

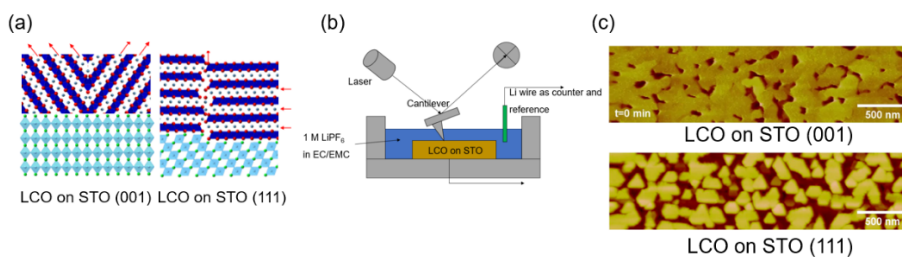


Figure 1 (a) Schematics showing the epitaxial growth of LCO on (001), and (111)-oriented STO substrates. (b) In-situ electrochemical AFM set up (c) Surface morphology of LCO films.

References

- (1) Qin, C.; Wang, L.; Yan, P.; Du, Y.; Sui, M. LiCoO₂ Epitaxial Film Enabling Precise Analysis of Interfacial Degradations. *Chinese Physics Letters* **2021**, *38* (6). <https://doi.org/10.1088/0256-307X/38/6/068202>.
- (2) Qin, C.; Jiang, Y.; Yan, P.; Sui, M. Revealing the Minor Li-Ion Blocking Effect of LiCoO₂ Surface Phase Transition Layer. *Journal of Power Sources* **2020**, *460*. <https://doi.org/10.1016/j.jpowsour.2020.228126>.
- (3) Yang, Z.; Ong, P. V.; He, Y.; Wang, L.; Bowden, M. E.; Xu, W.; Droubay, T. C.; Wang, C.; Sushko, P. v.; Du, Y. Direct Visualization of Li Dendrite Effect on LiCoO₂ Cathode by In Situ TEM. *Small* **2018**, *14* (52). <https://doi.org/10.1002/sml.201803108>.

September 9, 2021 (Thursday) 16:55-17:10

Cu-Ga-S/ZnS Quantum Dots with Silica Melting Gel as a Luminescent Downshifting Coating for Enhancing Solar Photovoltaic Power Generation

Si-Hao Chen, Xu Han, Changqing Pan and Chih-hung Chang

Corresponding Author: Chih-Hung.Chang@oregonstate.edu

School of Chemical, Biological and Environmental Engineering, Oregon State University, Corvallis, OR 97331

Cu-Ga-S/ZnS core-shell quantum dots (CGS/ZnS QDs) are a luminescent downshifting material that displays excellent optical properties and great stability and contains no toxic elements such as Cd or Pb. CGS/ZnS QDs can efficiently absorb UV photons then emit a broad band of visible photons with a significant Stokes shift around 209 nm. In this study, CGS/ZnS QDs were synthesized by the hot-injection method. Their optical properties were tuned by controlling the Cu/Ga precursor molar ratio and reaction time. UV-Vis absorption spectroscopy and photoluminescence (PL) spectroscopy were used to study the spectral absorption and emission. The crystal structure of QDs was characterized by X-ray diffraction. The particle size, size distribution, and shape of the QDs were determined using high-resolution transmission electron microscopy. CGS/ZnS QDs mixed with silica melting gels that flow easily at room temperature and consolidate at 170 °C to make the QD-doped melting gel coatings on the glass. These coatings can become a cost-effective and convenient strategy to improve the efficiency of solar cells without altering the existing cell manufacturing processes. QD-doped melting gel coatings with different concentrations were put on top of the solar cell's cover glass and tested for their efficacy using a solar simulator. The results show that the coatings can improve the efficiency of polysilicon solar cells.

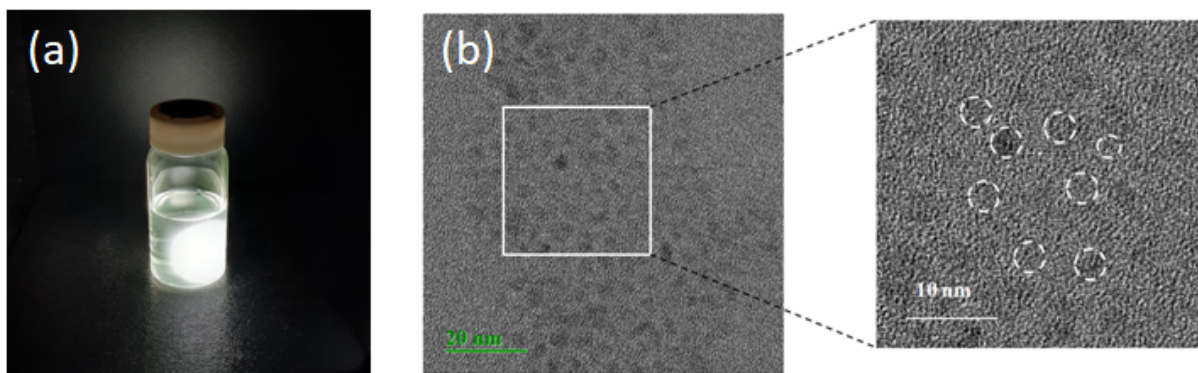


Figure 1 (a) Image under the UV 360 nm flashlight and (b) TEM image of Cu-Ga-S/ZnS quantum dots with the Cu/Ga molar ratio of 1/8

References:

[1] Jalalah, M.; Al-Assiri, M. S.; Park, J.-G. One-Pot Gram-Scale, Eco-Friendly, and Cost-Effective Synthesis of CuGaS₂/ZnS Nanocrystals as Efficient UV-Harvesting Down-Converter for Photovoltaics. *Adv. Energy Mater.* **2018**, 8 (20), 1703418. <https://doi.org/10.1002/aenm.201703418>.

[2] Klein, L. C.; Jitianu, A. Organic-Inorganic Hybrid Melting Gels. *J. Sol-Gel Sci. Technol.* **2010**, 55 (1), 86–93. <https://doi.org/10.1007/s10971-010-2219-4>.

September 9, 2021 (Thursday) 17:10-17:25

Capturing the Coverage Dependence of Aromatics via Mean-Field Models

Naseeha Cardwell¹, Alyssa J. R. Hensley^{1,2}, and Jean-Sabin McEwen¹

Corresponding Authors: ahensley@stevens.edu, js.mcewen@wsu.edu

¹ The Gene and Linda Voiland School of Chemical Engineering and Bioengineering, Washington State University, Pullman, Washington 99164, United States

² Department of Chemical Engineering & Materials Science, Stevens Institute of Technology, Hoboken, New Jersey, 07030, United States

Hydrodeoxygenation, the process in which oxygen is removed from biomass-derived products (represented here as oxygenated aromatics), occurs via catalytic hydrogenation and C-O bond cleavage. Critically, many models capturing the reaction pathways lack inclusion of coverage effects, decreasing the accuracy of the predicted dominant pathways and the rate limiting steps. Here, we determine the effect of coverage on the adsorption energies of a range of oxygenated aromatics (i.e. benzene, phenol, etc.) on Pt(111) and Ru(0001) using density functional theory (DFT) with van der Waals effects included.

From this study, we have derived three key insights into the coverage dependence of oxygenated aromatics. First, from Figure 1A, we see that closed shell adsorbates (i.e. benzene, phenol, anisole, etc.) have significant repulsive interactions (i.e. adsorption energy weakens with increasing coverage), whereas adsorbates with free radicals, i.e. phenoxy, have comparatively flat mean-field (MF) slopes, indicating that there are minimal coverage effects for these systems. Second, increasing the size of the aromatic functional group from hydroxyl (phenol) to methoxyl (anisole) results in an increase in the MF slope by ~50%, demonstrating that the change in functional group can significantly increase the repulsive lateral interactions in the system. Third, MF slopes for all adsorbates are 2-7 times higher on Pt(111) compared to Ru(0001), which suggests that the adsorbate-metal interaction (compared to adsorbate-adsorbate interactions) governs the lateral interactions for Pt and that higher oxygenated adsorbate coverages are likely on Ru(0001).

Using our database of adsorption energies versus coverage, we determined predictors for the coverage dependent behavior of oxygenated aromatics on transition metal surfaces. Specifically, we found that the MF slopes of the adsorption energies are linearly dependent on the adsorbed system work function (Figure 1B). This simple, mathematical relation enables the rapid prediction of coverage dependent behavior of oxygenated aromatics on transition metal surfaces, significantly decreasing the computational cost to incorporate such effects into kinetic models.

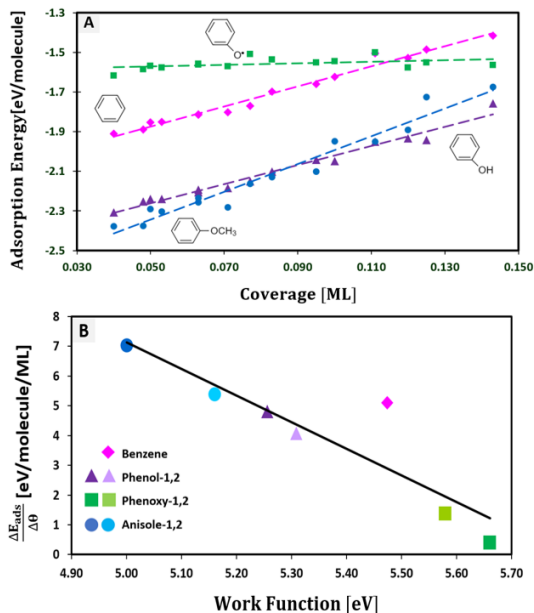


Figure 1 **A** Binding energy as a function of increasing coverage for aromatics on Pt(111). We remark here that the adsorption energies for phenoxy are defined here with respect to phenol and molecular hydrogen in the gas phase. **B** Work function of aromatics plotted against the adsorption energy slope as a function of changing coverage. 1 (darker shade) refers to the more favorable bridge site; 2 (lighter shade) refers to the top site. Work functions are calculated at the lowest coverage of 0.04 ML.

September 9, 2021 (Thursday) 17:25-17:40

Characterization of the composition and mechanical properties of aprismatic crocodilian tooth enamel

Jack Grimm^{1*}, Cameron Renteria^{1*}, and Dwayne Arola^{1,2,3}

Corresponding Author: darola@uw.edu

¹. Department of Materials Science and Engineering, University of Washington Seattle, WA USA.

². Department of Restorative Dentistry, School of Dentistry, University of Washington Seattle, WA USA

³. Department of Mechanical Engineering, University of Washington Seattle, WA USA

*Graduate student

Tooth enamel is a remarkably resilient biological material. It is the hardest tissue in the body yet still exhibits extraordinary damage tolerance. Previous studies have attributed this behavior to a complex hierarchical microstructure, mineralogical variations, and gradients in composition throughout the enamel thickness. A distinct aspect of the meso-scale structure in mammalian enamel is decussation, a complex weaving pattern of rods of aligned hydroxyapatite mineral nanocrystals. Reptilian enamel is “aprismatic,” meaning the mineral nanocrystals are not assembled into rods. This removes a critical level of hierarchical microstructure needed for damage tolerance. However, crocodylians, including the American alligator and the saltwater crocodile, are capable of exerting bite forces much greater than mammals, yet research characterizing their enamel is scant. This study investigates the microstructure, composition, and mechanical performance of crocodylian enamel in comparison to human enamel. It is hypothesized that underlying enamel formation mechanisms result in similar gradients in both human and crocodylian enamel, but that the less complex crocodylian microstructure yields unique mechanical properties to compliment crocodylian polyphyodont tooth regeneration.

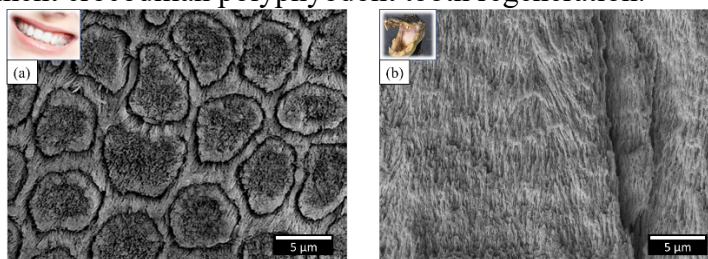


Figure 1. (a) Micron-scale rods in human enamel, consisting of bundles of aligned hydroxyapatite mineral nanocrystals. (b) Hydroxyapatite nanocrystals in the aprismatic enamel of an American alligator.

September 9, 2021 (Thursday) 17:40-17:55

Aerosol properties and processing during wintertime under hazy condition

Susan Mathai¹, Zhezhen Cheng², Amna Ijaz³, Nurun Nahar Lata⁴, and Swarup China⁵

Corresponding Author: smathai@mtu.edu, Zezen.cheng@pnnl.gov, aijaz@mtu.edu, nmlata@mtu.edu, Swarup.china@pnnl.gov.

¹ Pacific Northwest National Laboratory, Environmental and molecular sciences laboratory, Richland, USA.

² Pacific Northwest National Laboratory, Environmental and molecular sciences laboratory, Richland, USA.

³ Pacific Northwest National Laboratory, Environmental and molecular sciences laboratory, Richland, USA.

⁴ Michigan Technological University, Physics Department, Houghton, USA.

⁵ Pacific Northwest National Laboratory, Environmental and molecular sciences laboratory, Richland, USA.

Atmospheric aerosols emitted into the atmosphere often as externally mixed compounds coagulate or condense on each other due to aging to exist in internally mixed state. Variability in mixing state of atmospheric aerosols play a major role in uncertainties associated with the estimated radiative forcing. Meteorological condition plays a major role in determining the mixing state of particles in the atmosphere. We collected samples during wintertime and under hazy condition

from a polluted region which is impacted by biomass burning from household activities and agricultural burning. The collected samples were analyzed using multi-modal micro-spectroscopy and chemical imaging techniques such as computer controlled scanning electron microscopy, transmission electron microscopy and scanning transmission X-ray microscopy/near edge X-ray absorption fine structure spectroscopy to determine the size resolved morphology and chemical composition of individual particles. Due to extensive fire activities during winter the K-rich particles are dominant in the atmosphere. We also observed an abundance of sulfates in the sample which could be the result of aqueous phase reaction due to regional haze. Furthermore, we investigated phase state of individual particles with and without inorganic inclusions and our results suggest that particles with inclusions are in semi-solid state while particles without inclusions are in solid-state. The results from this study will help in understanding different mixing state of particles in an urban polluted region and the impact of mixing states on particle phase state.

September 10, 2021 (Friday) Morning

Session 7: Energy Applications II. Chair: Chih-hung Chang

September 10, 2021 (Friday) 8:30-9:10

Deciphering electronic and geometric effects in bimetallic catalysis for biomass upgrading (Invited)

Konstantinos Goulas¹

¹*School of Chemical, Biological and Environmental Engineering, Oregon State University, Corvallis, OR 97331*

Abstract:

The successful implementation of the biorefinery concept requires the development of pathways to produce a broad range of fuels and chemicals from biomass. Key to achieving high selectivity in tandem dehydrogenation-aldol condensation reactions is the prevention of decarbonylation reactions of the reactive aldehyde intermediates. Cu overlayers on Pd prevent the binding of carbonyl alkyl species onto the surface, thereby preventing decarbonylation. At the same time, desirable dehydrogenation reactions are promoted by electron donation from Cu to Pd, rendering Cu significantly more active. We use this insight to develop an active, selective and stable catalyst system to produce biofuel precursors.

September 10, 2021 (Friday) 8:10-9:25

Effects of aprotic and polar co-adsorbates on C-OH and O-H bond cleavages on Pd (111)

Kingsley Chukwu^a and Líney Árnadóttir^a

^a*School of Chemical, Biological and Environmental Engineering, Oregon State University, Corvallis, OR, 97331, United States.*

Theoretical and experimental studies have shown that co-adsorbates and solvents influence the selectivity and rate of heterogeneous catalytic reactions by influencing the energetics of different bond cleavages. Fundamental understanding of how protic and aprotic polar co-adsorbates affect different bond cleavages will give us valuable insight into how co-adsorbates affect the reaction mechanism, rate and selectivity of catalytic reactions. Here we present a density functional theory (DFT) calculation of how protic (water and methanol), and aprotic (dimethyl sulfoxide, acetonitrile and acetone) polar co-adsorbates affect the C-OH and O-H bond cleavage of acetic acid intermediates during acetic acid decomposition over Pd (111). Our results suggest that co-adsorbed water and methanol favors O-H bond cleavage over C-OH bond cleavage. While co-adsorbed acetonitrile and acetone makes C-OH bond cleavage more competitive with O-H bond cleavage by inhibiting O-H bond cleavage, but dimethyl sulfoxide enhances both C-OH and O-H bond cleavages. These calculations give insights into how different co-adsorbates affect bond cleavages differently, which can lead to changes in selectivity and reaction rate.

September 10, 2021 (Friday) 9:25-9:40

Understanding the Electronic Structure Evolution of Epitaxial $\text{LaNi}_{1-x}\text{Fe}_x\text{O}_3$ Thin Films for Water Oxidation

Le Wang¹, Prajwal Adiga², Widitha S. Samarakoon², Kelsey A. Stoerzinger², Mark E. Bowden³, Peter V. Sushko¹, Zhenxing Feng², Yingge Du¹, and Scott A. Chambers¹

¹Physical and Computational Sciences Directorate, Pacific Northwest National Laboratory, Richland, Washington 99354, USA

²School of Chemical, Biological and Environmental Engineering, Oregon State University, Corvallis, Oregon 97331, USA

³Environmental Molecular Sciences Laboratory, Pacific Northwest National Laboratory, Richland, Washington 99352, USA

Abstract: Rare earth nickelates including LaNiO_3 are promising catalysts for water electrolysis to produce oxygen gas. Recent studies report that Fe substitution for Ni can significantly enhance the oxygen evolution reaction (OER) activity of LaNiO_3 . However, the role of Fe in increasing activity remains ambiguous, with potential origins both structural and electronic in nature. Based on a series of epitaxial $\text{LaNi}_{1-x}\text{Fe}_x\text{O}_3$ thin films synthesized by molecular beam epitaxy, we report that Fe substitution tunes the Ni oxidation state in $\text{LaNi}_{1-x}\text{Fe}_x\text{O}_3$ and a volcano-like OER trend is observed with $x = 0.375$ being the most active. Spectroscopy and ab initio modeling reveal that high-valent $\text{Fe}^{3+\delta}$ cationic species strongly increase the transition metal (TM) $3d$ bandwidth via Ni-O-Fe bridges and enhance TM $3d$ -O $2p$ hybridization, boosting the OER activity. These studies deepen our understanding of structural and electronic contributions that give rise to enhanced OER activity in perovskite oxides.

September 10, 2021 (Friday) 9:40-9:55

Inkjet-Printed p-type $\text{CuBr}_x\text{I}_{1-x}$: A Wide-Range-Tunable Resistivity of wearable thin-film transistors

Shujie Li¹, Brayden Liebe¹, Changjin, Song², Shelby, Surprens¹, Skip, Rochefort¹, Sangwoo Lim² and Chih-Hung Chang¹

Corresponding Author: Chih-Hung.Chang@oregonstate.edu

¹. Department of Chemical Engineering, Johnson Hall, Oregon State University, Corvallis, Oregon-97331, USA

². Department of Chemical and Biomolecular Engineering, Yonsei University 50 Yonsei-ro, Seodaemun-gu, Seoul 03722, Republic of Korea

The high hole density of copper iodide hinders its performance and restrict the on/off ratio as a complementary p-type TFTs. [1] Alternatively, the CuBrI alloy provides a way of widely resistance tunability [2] and optical transparency, leading to the improved gate modulation and on/off ratio, which was confirmed by the electrical and optical characterization, such as, XRD, SEM, and XPS in this work. Therefore, based on the stable and printable ink from binary metal halide salts that undergo the solute dissolution and re-crystallization into dense CuBrI thin film

after printing, a low-temperature synthesis of p-type CuBrI thin film transistor was firstly demonstrated through inkjet printing technology. By adjusting the CuI/CuBr ratios, the hole density/conductivity of CuI was successfully reduced, resulting a improved device performance with highest saturation mobility of 6.57 cm²/Vs and an average On/Off ratio of 10³–10⁵. Finally, attributing to the surface passivation and selection of low temperature PVA dielectric layer, the textile-based CuBrI thin film transistor was reported showing the typical output curves with field-effect mobility of 0.45 cm²/Vs, which indicates a potential application for printed wearable complementary circuits

References:

- [1] Choi, C., Gorecki, and Chang, C. Low-temperature, inkjet-printed p-type copper(i) iodide thin-film transistors. *Journal of Materials Chemistry C*, 4(43), 2016, pp.10309-10314.
- [2] Yamada, N, Tanida, Y, Yoshida, S. Wide-Range-Tunable p-Type Conductivity of Transparent CuI_{1-x}Br_x Alloy. *Advanced Functional Material*, 30(34), 2020, 2003096

September 10, 2021 (Friday) 9:55-10:10

Making electrodes by particle stamping for microscopic and electrochemical analysis

Jiyoung Son,¹ Xiao-Ying Yu,¹ Shawn L. Riechers,¹ and Edgar C. Buck¹

Corresponding Author: xiaoying.yu@pnnl.gov

¹. Energy and Environment Directorate, Pacific Northwest National Laboratory, WA 99354, USA.

Studying the electrochemical behavior of nanoparticles using electron microscopy techniques is challenging due to the difficulty in fabricating the working electrode (WE) containing nanoparticles with a consistent loading of particles of interest while minimizing the background signal from the substrate. In this paper, we describe a new nanoparticle stamping method to prepare electrodes contained within a microfluidic platform that are suitable for *in-operando* electron microscopy [1, 2]. Microscopic and microanalysis techniques, including atomic force microscopy (AFM) and time-of-flight secondary ion mass spectrometry (ToF-SIMS), were used to characterize the as-fabricated electrodes; and electrochemical analysis was used to verify electrode performance.

The electrodes with attached particles were fabricated as a part of the established microfluidic device for multimodal spectroscopy and microscopy of liquids [1, 2], which is called the System for Analysis at the Liquid-Vacuum Interface Electrochemical cell (SALVI E-cell). Approximately 20 mg cerium oxide nanoparticles (CeO₂, US research materials Inc, 10 nm mean diameter) were used in each device. Lower mass loadings are possible.

Cyclic voltammetry (CV) scans (Figure 1C) of the fabricated device using the sequence stamping approach shows the unique electrochemical profiles of CeO₂ nanoparticles [3]. This result was different from that of the conductive epoxy control CV shown in Figure 1D. For example, there were unique CV peak profiles at -0.1 V (from 1 V to -1 V scan) and 0.7 V (from -1 V to 1 V scan),

showing different features from the control CV profile. Moreover, we characterized the stamped electrode surfaces using AFM and ToF-SIMS via 2D imaging shown in Figure 2. AFM images (Figure 2A-D) show the morphology of nanoparticle aggregation on the stamped surface ranging from 40 to 130 nm in height and the ToF-SIMS 2D image (Figure 2E) verifies the presence of CeO₂ particles on the stamped surface. Both microanalysis and imaging techniques provided valuable insights for optimization and assisted method development. Nanomaterials can be analyzed relatively conveniently to study their electrochemical properties using this new particle attachment method in a microfluidic cell. We provide a new tool for rapid nanomaterial electrochemical analysis. More importantly, this approach permits in situ SEM analysis and imaging and allows nanoparticle electrochemical performance evaluation using multi-dimensional microanalysis.

September 10, 2021 (Friday) 10:10-10:30

Break

Session 8: Biology and Environmental Study II. Chair: Vaithiyalingam Shutthanandan

September 10, 2021 (Friday) 10:30-11:10

Chemical imaging of atmospheric particles from wildfire smoke (Invited)

Swarup China¹

Corresponding Author: swarup.china@pnnl.gov

¹. Pacific Northwest National Laboratory, WA 99354, USA.

Atmospheric particles directly affect our planet's radiation budget by scattering and absorbing solar radiation, and indirectly by interacting with clouds. Biomass burning such as wildfire is one of the largest sources of carbonaceous aerosols in the atmosphere, significantly affecting earth's radiation budget and climate. Carbonaceous particles can alter their morphology, can oxidize and mix, and can become coated by organic and inorganic materials during atmospheric processing. The morphology and mixing state of absorbing aerosol play an important role in determining their optical properties and radiative properties. Chemical imaging techniques using multi-modal methodologies provide critical information about formation, growth, and evolution of aerosol in the atmosphere. I will discuss how chemical imaging of wildfire aerosol provides important insights into the atmospheric chemistry.

September 10, 2021 (Friday) 11:10-11:25

Objective crystallographic symmetry classifications of atomic and molecular resolution images from crystals in direct and Fourier space

Peter Moeck, pmoeck@pdx.edu

Department of Physics, Portland State University, Portland, Oregon, USA.

A geometric form of information theory allows for objective classifications of the crystallographic [1,2] and quasicrystallographic symmetries in noisy digital images. Such classifications are based solely on the image pixel intensity values, justifiable assumptions about the aggregate distribution of generalized noise in the images, asymptotic extrapolations to zero-noise images, and rational symmetry model selections with maximized predictive accuracy in the presence of both symmetry-inclusion relations and pseudo-symmetries. Preferring a well developed geometric form of information theory over a theoretically possible geometric-Bayesian approach for these classifications is the only subjective choice made. Assuming approximately Gaussian distributed generalized noise, objective crystallographic and quasicrystallographic symmetry classifications can be made for noisy images from both scanning probe and transmission electron microscopes in direct and Fourier space. A binary type classification of structurally very similar materials into either a decagonal quasicrystal or one of its rational/crystalline approximants is provided here based on the approximate point symmetries in their electron diffraction spot patterns (EDSPs), Fig. 1.

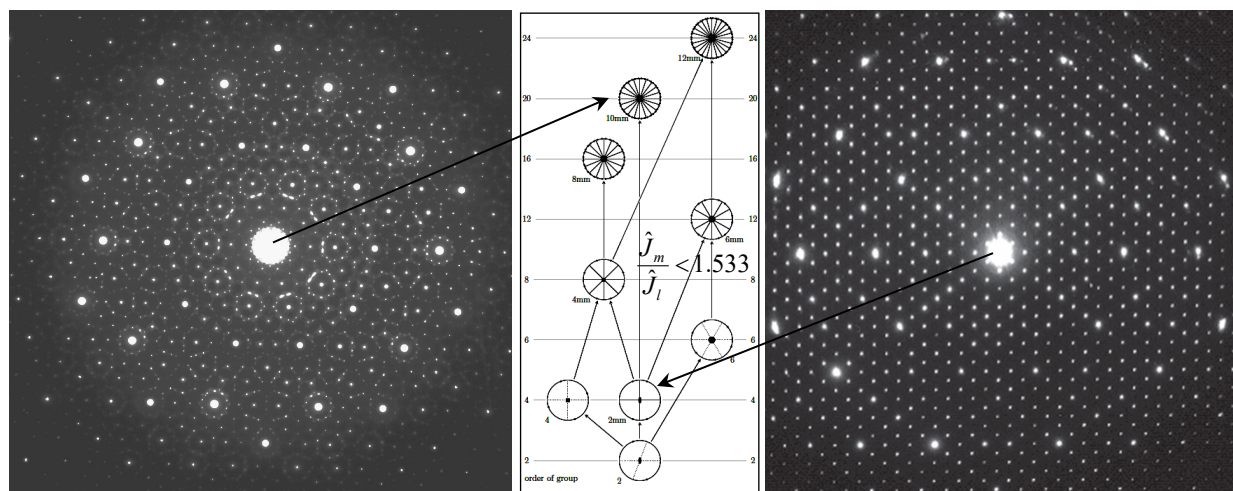


Figure 1 (a) EDSP of $\text{Al}_{69.7}\text{Co}_{10.0}\text{Ni}_{20.3} \pm 0.2$ atom percent (thanks to Prof. Dr. Peter Gille of Ludwig Maximilian University of Munich). (b) 2D point symmetry hierarchy of EDSPs. (c) EDSP of $\text{Al}_{71.5}\text{Co}_{16}\text{Ni}_{12.5}$ (in open access). Arrows point to the respective point symmetries. The maximal allowance of the ratio of the sums of squared spot intensity residuals for the transition from point group $2mm$ to point group $10mm$ is also given in (b).

References:

- [1] P. Moeck, Towards generalized noise-level dependent crystallographic symmetry classifications of more or less periodic crystal patterns, *Symmetry* 10 (2018) 133.
- [2] P. Moeck, Objective crystallographic symmetry classifications of noisy and noise-free 2D periodic patterns with strong Fedorov type pseudosymmetries, arXiv: 2108.00829, (23 pages, July 22, 2021), shortened version submitted to *Acta Crystallographica A*.

September 10, 2021 (Friday) 11:25-11:40

Revealing the material interface compatibility between CO₂ separation membrane and water-lean solvents using ToF-SIMS

Jun Gao¹, Yuchen Zhang¹, Jiyoung Son¹, Jason E. Baron², David J. Heldebrant², Roger Rousseau³, and Xiao-Ying Yu*¹

*Corresponding author email: xiaoying.yu@pnnl.gov

¹ Energy and Environment Directorate, Pacific Northwest National Laboratory, Richland, WA 99354

² Department of Chemical and Biological Engineering, The University of Alabama, Tuscaloosa, AL, 35487

³ Physical Science Division, Pacific Northwest National Laboratory, Richland, WA, 99352

Water-lean solvents are considered as a promising technology for carbon dioxide (CO₂) capture. Such CO₂ capture molecules include but not limited to N-(2-ethoxyethyl)-3-morpholinopropan-1-amine (2-EEMPA), 3-methoxy-N-(pyridine-2-ylmethyl)propan-1-amine (MPMPA), and 1-((1,3-Dimethylimidazolidin-2-ylidene)amino)propan-2-ol (IPADM-2-BOL). To better integrate these solvents with the CO₂ separation process for direct air capture of CO₂, it is necessary to understand the chemical compatibility with CO₂ separation membranes. Characteristic peaks of water-lean solvents and separation membrane were observed using time-of-flight secondary ion mass spectrometry (ToF-SIMS) using the static mode. For example, m/z^+ C₁₁H₂₅N₂O₂⁺, m/z^+ C₁₀H₁₇N₂O⁺, m/z^+ C₈H₁₈N₃O⁺, and m/z^+ 263 C₁₆H₁₁N₂O₂⁺ are the protonated EEMPA, protonated MPMPA, protonated IPADM-2-BOL, and the fragment of CO₂ separation membrane, respectively, showing the power of molecular detection of ToF-SIMS. In addition, in the interface of separation membrane, a synthesized PEEK material, with EEMAP and IPADM-2-BOL, respectively, new characteristic peaks were observed in high mass range with some low mass range peaks disappeared, indicating new species formed during the interactions between the CO₂ separation membrane and water-lean solvents, such as EEMPA and IPADM-2-BOL. Interestingly, fewer new peaks formed in the interface between the CO₂ separation membrane and MPMPA, suggesting potentially better chemical compatibility of MPMPA than EEMPA and IPADM-2-BOL. Our results show that ToF-SIMS can be a useful tool to study the interface between the candidate CO₂ separation membrane and water-lean solvents at the molecular level, providing insights into the design of direct air capture devices.

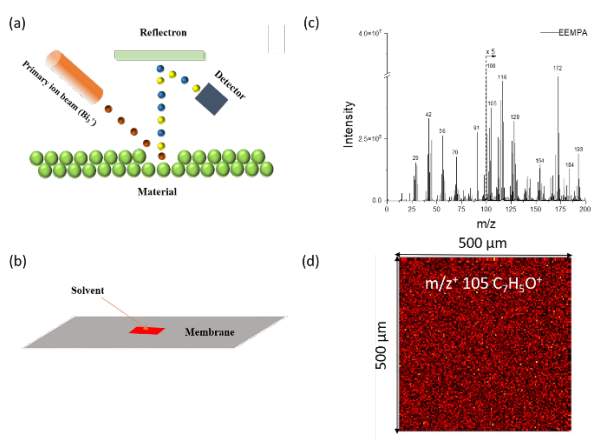


Figure 1. The schematic of ToF-SIMS: (a) working principle of ToF-SIMS; (b) a photo of sample preparation; (c) a static SIMS mass spectrum; and (d) a 2D image from static ToF-SIMS.

September 10, 2021 (Friday) 11:40-11:55

TBD

Lyndi E. Strange¹, and Xiao-Ying Yu*¹

*Corresponding author email: xiaoying.yu@pnnl.gov

¹. Energy and Environment Directorate, Pacific Northwest National Laboratory, Richland, WA 99354

September 25, 2020 (Friday) 11:55-12:40

Award ceremony and closing remarks